

UNCLASSIFIED

SECURITY CLASSIFICATION OF THIS PAGE (When Data Entered)

REPORT DOCUMENTATION PAGE		READ INSTRUCTIONS BEFORE COMPLETING FORM
1. REPORT NUMBER HDL-TR-2058	2. GOVT ACCESSION NO.	3. RECIPIENT'S CATALOG NUMBER
4. TITLE (and Subtitle) The Fluidic Approach to Mud Pulser Valve Design for Measurement-While-Drilling Applications		5. TYPE OF REPORT & PERIOD COVERED Technical Report
		6. PERFORMING ORG. REPORT NUMBER
7. AUTHOR(s) Allen B. Holmes		8. CONTRACT OR GRANT NUMBER(s) PRON: WD3-174 OWDA9
9. PERFORMING ORGANIZATION NAME AND ADDRESS Harry Diamond Laboratories 2800 Powder Mill Road Adephi, MD 20783-1197		10. PROGRAM ELEMENT, PROJECT, TASK AREA & WORK UNIT NUMBERS Program Ele: M
11. CONTROLLING OFFICE NAME AND ADDRESS Department of Interior Minerals Management Service Reston, VA 22091		12. REPORT DATE November 1985
		13. NUMBER OF PAGES 53
14. MONITORING AGENCY NAME & ADDRESS (if different from Controlling Office)		15. SECURITY CLASS. (of this report) UNCLASSIFIED
		15a. DECLASSIFICATION/DOWNGRADING SCHEDULE
16. DISTRIBUTION STATEMENT (of this Report) Approved for public release; distribution unlimited. This work was sponsored by the Department of Interior, Minerals Management Service, Reston, VA 22091.		
17. DISTRIBUTION STATEMENT (of the abstract entered in Block 20, if different from Report)		
18. SUPPLEMENTARY NOTES HDL Project: 315334 MIPR: 3-6035-25213		
19. KEY WORDS (Continue on reverse side if necessary and identify by block number) Measurement while drilling MWD Pulser Mud pulser		
20. ABSTRACT (Continue on reverse side if necessary and identify by block number) The design and operation are described for three fluidic-type mud pulsing valves. In principle, these valves employ centrifugal pressure forces in a confined vortex flow field to throttle the fluid (mud), which circulates through a drill pipe. Valves of this type can be used for transmitting diagnostic information in the form of binary coded pressure pulses. The pulses travel through the drilling mud between the drill bit and the surface while the well is being drilled.		

DD FORM 1473 1 JAN 73 EDITION OF 1 NOV 65 IS OBSOLETE

UNCLASSIFIED

1 SECURITY CLASSIFICATION OF THIS PAGE (When Data Entered)

20. ABSTRACT (Cont'd)

The report discusses the theoretical and simulated operation of vortex valves in a circulating mud system. Test data are presented which describe the steady flow and transient discharge characteristics of valves operating in a flow loop. The test data cover a flow range between 200 and 500 gal./min and a pulse frequency range between 1 and 10 Hz.

CONTENTS

	<u>Page</u>
1. INTRODUCTION	7
2. DESCRIPTION AND THEORY OF VORTEX VALVE OPERATION	9
2.1 Fluidic Mud Pulser Design Approaches	12
2.1.1 Fluid-Amplifier-Driven Vortex Valves	13
2.1.2 Tab-Actuated Vortex Valves	14
2.2 Use of Fluidic Vortex-Type Valves in a Mud Pulsing Circuit	15
3. EXPERIMENTAL PROGRAM	16
3.1 Flow Models	16
3.2 Test Fluids	22
3.3 Test Setups	22
4. RESULTS	26
5. SUMMARY AND CONCLUSIONS	33
6. RECOMMENDATIONS	33
ACKNOWLEDGEMENTS	34
SYMBOLS AND ABBREVIATIONS	35
LITERATURE CITED	36
SELECTED BIBLIOGRAPHY	37
DISTRIBUTION	51

APPENDICES

A.--THEORETICAL RELATIONSHIPS BETWEEN VORTEX VALVE PORT AREA, TURNDOWN RATIO, SIGNAL PRESSURE, and AVERAGE PRESSURE DROP	39
B.--FLUIDIC PULSER ASSEMBLY DRAWINGS, MODELS TAB-3 AND TAB-4	47

FIGURES

1. System layout of mud pulse telemetry	7
2. Configuration of vortex mud pulser valve	9

FIGURES (Cont'd)

	<u>Page</u>
3. Vortex valve parameters	9
4. Throttling characteristics of vortex valve	10
5. Fluid-amplifier-driven vortex valve	13
6. Operation of fluid-amplifier-driven vortex valve with radial and tangential inlets	14
7. Operation of fluid-amplifier-driven valve with tangential inlets	14
8. Tab-actuated vortex valve	14
9. Operation of tab-actuated vortex valve	15
10. Arrangement of four fluid-amplifier-driven vortex valves in drill pipe	15
11. Amplifier-driven vortex valves, model AMP-1	17
12. Amplifier-driven vortex valves, model AMP-2	18
13. Solenoid actuator used in vortex valve, model AMP-2	18
14. Tab-actuated vortex valves, model TAB-1	19
15. Tab-actuated vortex valves, model TAB-3	20
16. Actuator components	20
17. Tab-actuated vortex valves, model TAB-4	21
18. Vortex valve components, model TAB-4	22
19. Drilling Research Laboratories, test setup	24
20. Drilling Research Laboratories, test setup: (a) control room, (b) mud pump, (c) model installation	25
21. Effective flow area versus flow rate data describing AMP-2 model operating with vortex flow and radial flow	26
22. Effective outlet area versus supply pressure calculated for model AMP-1 operating with vortex and radial flow	26

FIGURES (Cont'd)

	<u>Page</u>
23. Effective outlet area versus flow rate calculated for model TAB-1 operating with vortex and radial flow	26
24. Photo sequence showing flow exhausting from fluid-amplifier-driven vortex valve with two tangential inlets (model AMP-1 T) during reversal of vortex	29
25. Response of AMP-2 pulser model to square-wave input signal when operating with water flowing at 300 gpm	30
26. Response of TAB-1 model to square-wave input signal	31
27. Response of TAB-3 model to continuous 6-Hz signal when operating with 12-ppg mud flowing at 300 gpm	31
28. Response of TAB-3 model to continuous 8-Hz square-wave input signal when operating with water flowing at 400 gpm	32
29. Response of TAB-4 model to single square-wave input pulse when operating with water flowing at 400 gpm	32
30. Response of TAB-4 model to variable frequency (DC to 10 Hz) input signal when operating on MUD VI at 300 gpm	32
31. Response of TAB-4 model to variable frequency input signal when operating with water flowing at 500 gpm	32

TABLES

1. Nozzle Dimensions	19
2. Mud Properties	23
3. Summary of Fluidic Pulser Test Data	27

1. INTRODUCTION

Measurements at the bottom of a well while drilling are now being transmitted between the drill bit and the surface using a technique called mud pulsing. Present operating systems transmit this information in the form of acoustic pulses or waves which travel through drilling mud* in the drill pipe at the speed of sound. Known chiefly as mud pulse or acoustic wave telemetry, this technique is being employed widely to provide measurements while drilling off-shore wells.¹

Figure 1 shows the layout of a typical pulsing measurement-while-drilling (MWD) system. In this system, pressure signals are produced by a mechanical device (pulsar) which throttles the circulating mud flow near the drill bit. Pressure signals are produced in the mud when ports in the pulsing device are mechanically covered and uncovered. A positive change in pressure is produced when the mud entering the pulsar slows down, and the pulse is ended when the flow velocity returns to its original level. The changing flow velocity produces a pressure wave which travels through the fluid up the drill pipe at the speed of sound (approximately 4800 ft/s in most drilling fluids). When they reach the surface, the signals are detected by a pressure transducer in

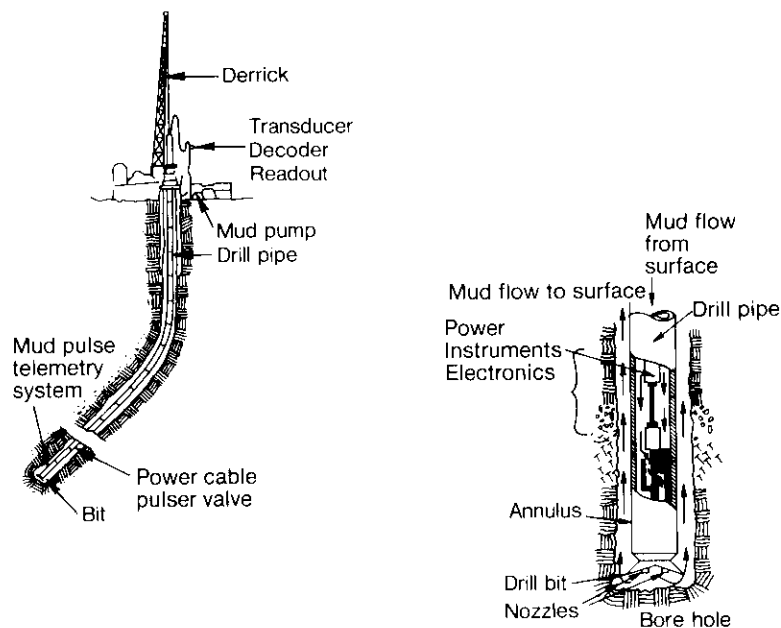


Figure 1. System layout of mud pulse telemetry (MWD).

¹Drilling Technology MWD Update: New Systems Operating, Oil and Gas Journal (17 March 1980).

*Drilling mud is a specially formulated fluid used while drilling, for cleaning the bottom of the hole and carrying formation cuttings to the surface, and for controlling pressures at the bottom of the well.

the wall of the drill pipe near the rig floor. The presence or absence of a pulse is commonly used to represent the binary numbers zero and one. A sequence of coded data bits carries information about conditions in the bottom of the well. This information is decoded electronically and displayed to the driller at the rig floor location.

The first complete mud pulse telemetry MWD system was put into commercial service by Teleco Oil Field Services in 1977.² This system records measurements of tool face angle, hole angle, and hole orientation while drill pipe is being added to the string. It then transmits these measurements after circulation is resumed. Teleco is reported to have used this system in drilling more than 1200 offshore wells.³ Several organizations have since entered the market and are providing similar services. Most measurement services are presently in the directional drilling area.^{4,5}

Principal advantages that mud pulsing has over other techniques (such as cables strung down the bore hole, insulated conductors in the wall of the drill pipe, electromagnetic transmissions through the formations, and sound waves in the wall of the drill pipe) are that it can be done with standard drill pipe and with very little impact on other drilling operations. However, the principal disadvantage which has limited the usefulness of mud pulsing is the relatively slow rate at which information is transmitted. Although present data transmission rates are high enough to transmit the types of measurements commonly used in directional drilling, they are not considered fast enough to transmit all the many additional types of information which would make it safer to drill more efficiently.

The maximum rate by which data can be transmitted by a mud pulser is essentially determined by the operating speed of the pulser and the acoustical transmissibility of the drilling fluid. At present, the fastest rate by which individual data bits are being transmitted through conventional drilling fluids from any reasonable depths (8,000 to 15,000 ft) is on the order of only between 40 and 80 bits per minute, depending on the system. Because many bits are required to represent a measurement (a minimum of 10 bits is required to represent a three-digit number in decimals), the maximum operating speed of pulsing mechanisms places a limit on the types of measurements which can be transmitted reliably. This, plus the poor acoustic properties of the drilling

²R. F. Spinnler and F. A. Stone, *Mud Pulse Logging While Drilling: Telemetry System Design, Development, and Demonstrations*, Teleco Oil Field Services, Inc., Transactions of the 1978 Drilling Technology Conference, International Association of Drilling Contractors (IADC), Houston, TX (March 1978).

³P. Seaton, Andrew Roberts, and L. Schoonover, *Drilling Technology Update: New MWD-Gamma System Finds Many Field Applications*, Oil and Gas Journal (21 February 1983), 80-83.

⁴Marvin Gearhart, *Mud Pulse MWD (Measurement-While-Drilling Systems)*, Society of Petroleum Engineers, SPE, 100053, 1980.

⁵Carl W. Buchholz, *Continuous Wave Mud Telemetry (The Analyst/Schlumberger) Proceedings, Technologies for MWD, Symposium, National Academy Press, Washington, DC (October 1981)*.

fluids, places an upper limit on the rate at which data can be transmitted from any reasonable depths. Although the present rates of data transmission are expected to increase, future improvements in pulser design and signal detection techniques are expected to be needed before the full advantages of higher data rate systems can be realized in practice.

Because of the enhanced safety which can be achieved through the use of measurements made while drilling, the Research and Development Program of the Offshore Operations Division of the Minerals Management Service (Department of Interior) initiated a program at the U.S. Army Harry Diamond Laboratories (HDL) to investigate the application of fluidic technology to the design of high-speed mud pulsers. The fluidic approach to mud pulser design is to throttle the drilling fluid using centrifugal pressure forces in a vortex rather than with moving parts. Several experimental fluid mud pulsing devices were designed, fabricated, and tested under simulated bore hole conditions during these investigations, and the results of these experiments are the subject of this report.

2. DESCRIPTION AND THEORY OF VORTEX VALVE OPERATION

The principal component used in a fluidic mud pulser is a vortex valve. Figure 2 shows the essential features of a vortex valve. Fluid dynamic parameters which govern the operation of vortex valves in general are described in figure 3.

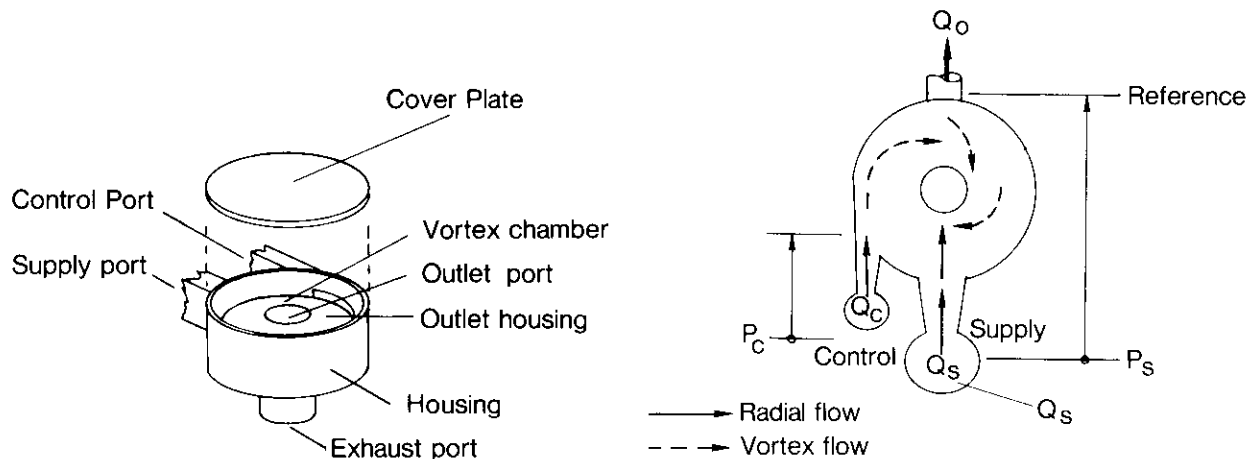


Figure 2. Configuration of vortex mud pulser valve.

Figure 3. Vortex valve parameters.

Basically, a vortex valve consists of a flat cylindrical chamber bounded on both ends by flat wall surfaces. Channels cut in the wall of the chamber serve as inlets for channeling the flow. A circular orifice directly in the center of the chamber forms the outlet. In the valve shown in figure 2, two

inlets are used to channel flow toward the center of the chamber and tangential to the axial centerline of the chamber. The number and arrangements of channels used to direct the supply and control fluids into the chamber depend upon how the vortex valve is to be used in a circuit.

For example, in the configuration shown in figures 2 and 3, when the radial inlet is pressurized and the control pressure is equal to zero, the fluid stream travels easily through the chamber and directly through the outlet. Since very little pressure is lost traveling this short distance, the total pressure drop in the chamber is low, and the major portion of the total pressure drop occurs in the outlet. Pressure-flow characteristics of a vortex valve with zero control are illustrated by the upper curve shown in figure 4.

When the control pressure level is increased above the pressure in the vortex chamber (see lines representing constant control pressures increasing toward the right in fig. 4), control flow is injected into the chamber which interacts with the supply flow. As the control pressure (and flow) is increased, momentum between the two streams is exchanged and a tangential velocity component is imparted to the fluid in the chamber. As fluid begins to rotate, a free vortex is formed in the chamber. In a free vortex, angular momentum of fluid is preserved and the angular velocity (V) of this fluid increases as it spirals toward the outlet. This change in velocity produces a corresponding change in the radial pressure gradient between the slower moving (high pressure) fluid at the outer radius of the chamber and the faster moving (low pressure) fluid near the center of the chamber. The change in pressure is a function of the change in velocity which occurs between the outer radius of the chamber (r_1) and the radius of the outlet (r_2). In a free vortex, this tangential velocity (V) component is

$$V_2 = V_1 \left(\frac{r_1}{r_2} \right)^n, \quad (1)$$

where $n = -1$ for a free vortex. Using V from equation 1, we express the change in pressure across the vortex as

$$dP = \frac{\rho V^2}{g} \frac{1}{r} dr, \quad (2)$$

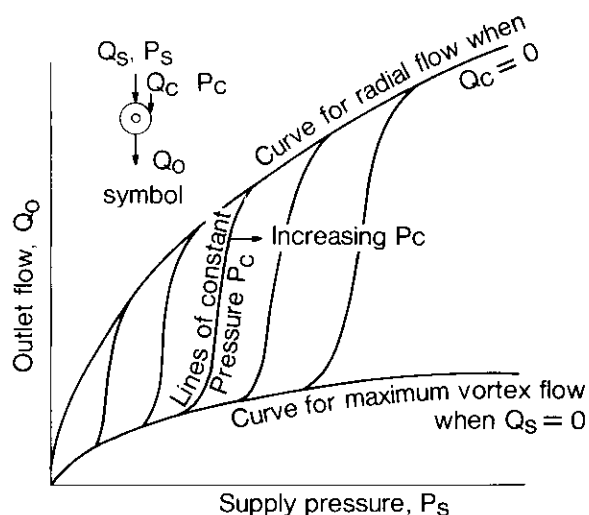


Figure 4. Throttling characteristics of vortex valve.

in which integration between radius (r_2) at the outlet and the radius of the chamber (r_1) gives the total radial pressure differential

$$\Delta P_2 = \frac{\rho V^2}{2n} \left(1 - \frac{r_2^{2n}}{r_1^{2n}} \right) . \quad (3)$$

Here ΔP_2 represents the radial pressure gradient caused by the vortex and produced between the inlet to the valve and the center of the chamber.

As pressure and flow in the control are increased, the supply flow is reduced and/or the supply pressure is increased. If the pressure across the chamber is held constant (as the control pressure is increased), the supply flow is reduced to zero, and only the control flow is exhausted from the chamber (see change in flow produced at constant pressure between curves, fig. 4). On the other hand, if the flow rate is held constant and the control pressure is increased, the supply pressure is increased (see change in pressure produced at constant flow between two curves shown in fig. 4).

Change in pressure produced at constant flow and change in flow produced at a constant pressure are the same as those which would be produced by reducing the area of an orifice. The change in pressure or flow can be equated to an area change when the operating pressure and flow rate are known. In practice, curves similar to those shown in figure 4 are generated while operating with radial and maximum vortex flow. Measured values of pressure and flow rate are then substituted into the Bernoulli equation and used to calculate equivalent flow areas for operation with radial and tangential flow. The equation used for the calculation is given as⁶

$$Q = A(2\Delta P/\rho)^{1/2} . \quad (4)$$

Solving equation 5 for the area term gives

$$A_2 = Q_2 / (2\Delta P_2 / \rho)^{1/2} , \text{ for radial flow,} \quad (5)$$

and

$$A_1 = Q_1 / (2\Delta P_1 / \rho)^{1/2} , \text{ for vortex flow,} \quad (6)$$

where ΔP = the total pressure drop across the vortex chamber, A = area of the outlet, ρ = density of the fluid, and subscripts 1 and 2 refer to operation in the vortex and radial flow modes.

The ratio between the effective outlet areas exhibited with radial and vortex flow in the chamber defines the turndown ratio:

$$\text{turndown ratio} = A_2 / A_1 .$$

²R. F. Spinnler and F. A. Stone, Mud Pulse Logging While Drilling Telemetry System Design, Development, and Demonstrations, Telco Oil Field Services, Inc., Transactions of the 1978 Drilling Technology Conference, International Association of Drilling Contractors (IADC), Houston, TX (March 1978).

⁶J. K. Vennard, Elementary Fluid Mechanics, 3rd Edition, John Wiley and Sons, NY (1954).

This ratio is a number commonly used to describe vortex valve performance. Principally, the turndown ratio is a function of chamber geometry. Past experimenters^{7,8} have shown that the turndown ratio increases with increasing radius ratio r_1/r_2 and decreases as the height of the chamber is reduced with respect to its radius as well as being affected by the relative width of the control inlet with respect to the radius of the chamber, etc. Turndown ratio has also been shown to decrease when the viscosity of the working fluid is increased. A complete discussion of the factors affecting turndown is contained in the references.

The flow resistance of a vortex valve operating without a vortex in its chamber can be expressed in terms of an area correction coefficient. This area correction coefficient (C_d) is defined as the ratio between the effective outlet area (A) measured without a vortex, given by the Bernoulli equation, and the actual area of the outlet nozzle. Knowledge of the area correction coefficient makes it possible to size a particular valve for operation in a drill pipe and to compare its discharge characteristics with other valves.

The response of a vortex valve is determined by the time required to produce the vortex. Past experimenters have shown the response time of a vortex valve to be directly proportional to the volume of the vortex chamber and inversely proportional to the average flow velocity through the chamber.^{7,8,9} Response times in general can be estimated by simply dividing the volume of the chamber by the average flow rate. However, in practice, viscous forces tend to retard formation of the vortex, which in turn tends to lengthen the actual response time.

2.1 Fluidic Mud Pulsar Design Approaches

Several methods for producing the vortex in a mud pulsar valve were considered during the course of these investigations. Basically, they centered upon the use of a fluid amplifier and a mechanically driven tab to produce vortex rotation. Specific problems addressed included the following:

(a) Could a strong vortex flow field be produced in a fluid with non-Newtonian properties similar to those found in most types of drilling fluids?

(b) Could the flow field be produced with a control pressure which is always equal to or less than the supply pressure?

(c) Could the vortex be produced reliably in a high pressure environment such as is normally encountered at the bottom of a bore hole while drilling?

⁷D. N. Wormley, *A Review of Diode and Triode Static and Dynamic Design Techniques, Massachusetts Institute of Technology, Proceedings of the 1974 Fluidic State-of-the-Art Symposium, Vol I, Harry Diamond Laboratories, Washington, DC.*

⁸S. S. Fineblum, *Vortex Diodes, State of the Art of Fluidics Symposium, Harry Diamond Laboratories (1974).*

⁹A. Holmes and S. Gehman, *Fluidic Approach to the Design of a Pulsar for Borehole Telemetry While Drilling, Harry Diamond Laboratories, HDL-TM-79-21 (August 1979).*

2.1.1 Fluid-Amplifier-Driven Vortex Valves

In the first method studied, a fluid amplifier is used to divert fluid between channels leading into the vortex valve. Figure 5 shows a conceptual drawing of the amplifier and its associated components. The basic idea is to use a small, fast-acting solenoid to control the operation of the amplifier and to use the output of the amplifier to control the direction of flow in the vortex chamber, as illustrated in figures 6 and 7.

In operation, fluid is supplied to the amplifier through the power jet nozzle. Here a jet flow is formed which attaches to and travels along one of two walls downstream of the nozzle. The side where attachment occurs depends upon which of the two amplifier control ports are pressurized. In the first circuit (fig. 6), the control ports are pressurized by fluid which passes through a spool valve. Pressurization of the left-hand control diverts the supply toward the right and produces a vortex flow; pressurization of the control on the right deflects the stream to the left and produces radial flow in the chamber. Flow directions are indicated by the arrows in figure 6. In the second circuit (fig. 7) actuating solenoids drive two diaphragms back and forth, which alternately forces fluid into and out of the amplifier controls. This, in turn, deflects the amplifier jet to the left and to the right as shown in the figure. The result produces clockwise and counterclockwise vortex rotation in the chamber. A valve of this type exhibits its lowest resistance to flow as the direction of flow reverses in the chamber.

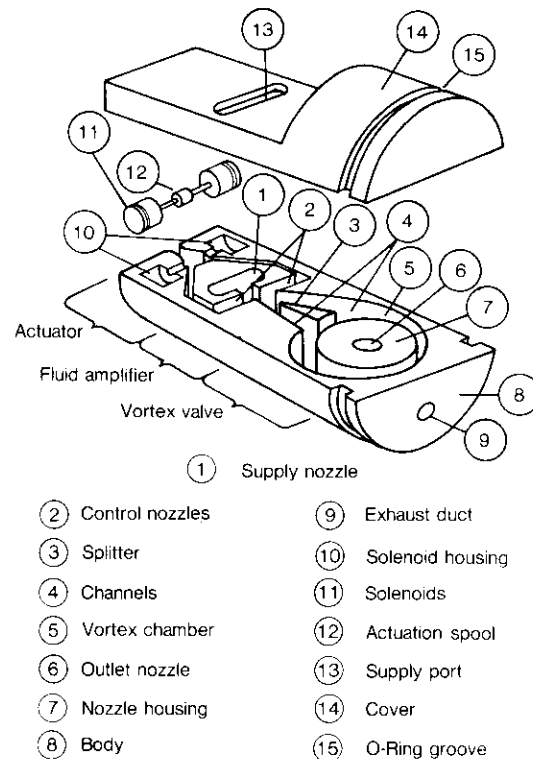


Figure 5. Fluid-amplifier-driven vortex valve.

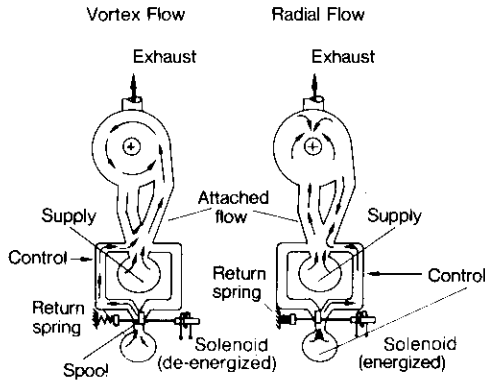


Figure 6. Operation of fluid-amplifier-driven vortex valve with radial and tangential inlets.

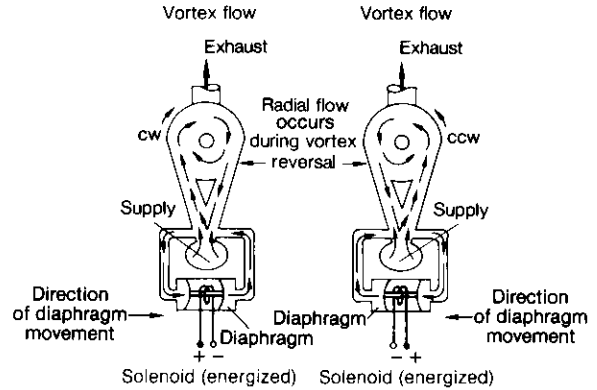


Figure 7. Operation of fluid-amplifier-driven valve with tangential inlets.

2.1.2 Tab-Actuated Vortex Valves

Figures 8 and 9 illustrate how a simple tab can be used to produce a vortex in a vortex valve. In operation, the solenoid moves the tab a short distance (approximately 0.10 in.) into and out of the vortex chamber as illustrated in figure 9. The presence of the tab prevents a symmetrical (radial) distribution of flow from taking place in the vortex chamber which, in turn, causes fluid to swirl through the chamber and produce a vortex. Returning the tab into the wall of the chamber restores the natural symmetry of the stream lines and eliminates the vortex.

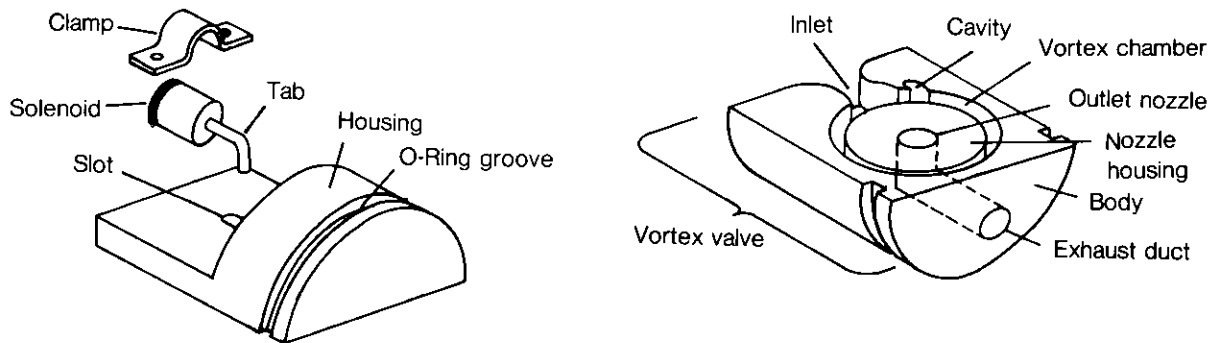


Figure 8. Tab-actuated vortex valve.

2.2 Use of Fluidic Vortex-Type Valves in a Mud Pulsing Circuit

Figure 10 shows how several vortex valves can be arranged in a drill pipe. When more than one vortex valve is used, the individual outlets are discharged in parallel. The capacity of the overall valve is a function of the size and number of outlet nozzles used. Response is governed by the volume of an individual chamber and by the volumetric flow rate through it. Using valves in parallel makes it possible to build high capacity mud pulsers without affecting response. A conceptual drawing showing the principal features of a fluidic mud pulser containing four vortex valves packaged in a drill pipe is shown in figure 10.

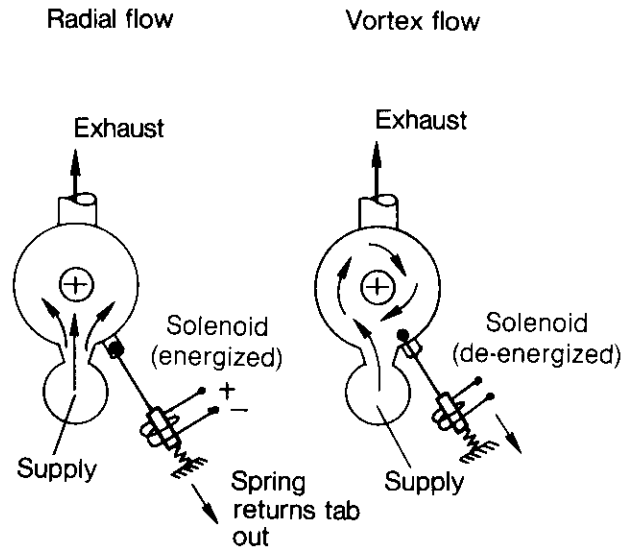


Figure 9. Operation of tab-actuated vortex valve.

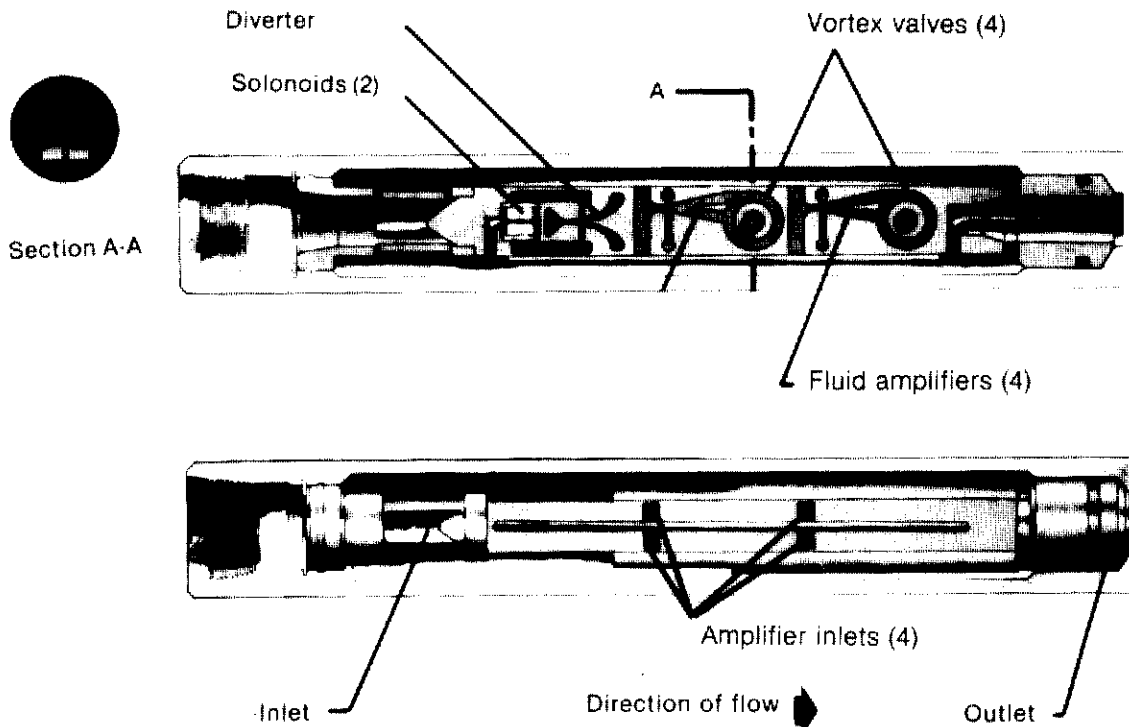


Figure 10. Arrangement of four fluid-amplifier-driven vortex valves in drill pipe.

The amplitude of pulses produced by a vortex-type mud pulsing valve is determined by the effective size of the valve (as determined by the effective area of the outlets) and the throttling action (turndown ratio) produced by the vortex. Flow equations describing the various relationships between operating turndown ratio and valve size and other drilling parameters (including drill bit nozzle size, pipe size, and circulating flow rate) are contained in appendix A.

3. EXPERIMENTAL PROGRAM

An experimental fluidic mud pulser test program was conducted. Objectives of the program were to see whether vortex-type valves would effectively throttle the types of fluids commonly used while drilling and what levels of turn-down and response could be produced by full-size operating devices.

The test program was conducted at HDL, Adelphi, MD, and at the Drilling Research Laboratories (DRL), Salt Lake City, UT. The following section describes the test hardware and tests which were conducted during the experimental portion of this program.

3.1 Flow Models

The first flow model contained a small amplifier-driven vortex valve equipped with radial and tangential inlets. Figure 11 shows the first flow model constructed. This model is brass and is held together with screws. The area of the outlet nozzles in the chamber is equal to 0.055 in.². The area of the power jet nozzles used in the amplifiers is equal to 0.040 in.². The areas the ports used in the model are considered to be approximately four times smaller than those required in a full-size device.

Figure 12 shows a model containing two full-size amplifier-driven vortex valves. This model is referred to as AMP-2. The area of the power jet nozzle used in each amplifier is equal to 0.50 in.² (1.0 × 0.50 in.). The areas and pertinent data on the nozzles used on the outlet side of the model are presented in table 1. The amplifiers were actuated by solenoids which moved (lower portion of the assembly) a slotted bar back and forth to cover and uncover ports leading to the control channels in the amplifier. Operation of the model and flow geometries employed is similar to that shown in figure 6. The principal parts of the solenoid mechanism used to actuate the model are shown in figure 13.

Figure 14 shows the first tab-actuated vortex valve that was built and tested. This unit is referred to as TAB-1. TAB-1 contains a vortex chamber with one inlet, cover plate, tab, outlet nozzle, and two solenoids with associated plunger assemblies. Dimensions of the nozzles used on the outlet side of the model are given in table 1. TAB-1 was made of aluminum and held together by screws. Actuator solenoids were secured to the outer wall of the model as shown in the figure. During a test, the model was mounted in the drill pipe housing used in previous tests. The pressure across the TAB-1 and AMP-2 models was monitored at the same locations, namely, in the wall of the drill pipe housing, midway between each end, and in the exhaust line leading from the outlet.



Figure 11. Amplifier-driven vortex valve, model AMP-1.

Three tab-actuated vortex valves are shown in figure 15. This valve assembly is referred to as TAB-3. The vortex valves used in this model are actuated by two solenoids housed in a pressure-compensated container at the forward end of the assembly. When energized, the solenoids move compressing a bellows which is attached to and moves the control rod. This in turn drives the three tabs into and out of the vortex chambers simultaneously. Materials used in this model principally include stainless-steel (series 303 and 304) for the housings, manifolds, and nozzle chamber assemblies, and carbon steel for the drill pipe housing. The overall assembly is 55 in. long, 6¹/₂ in. in diameter, and weighs approximately 350 lb. A detailed assembly drawing of this unit is shown in appendix B.

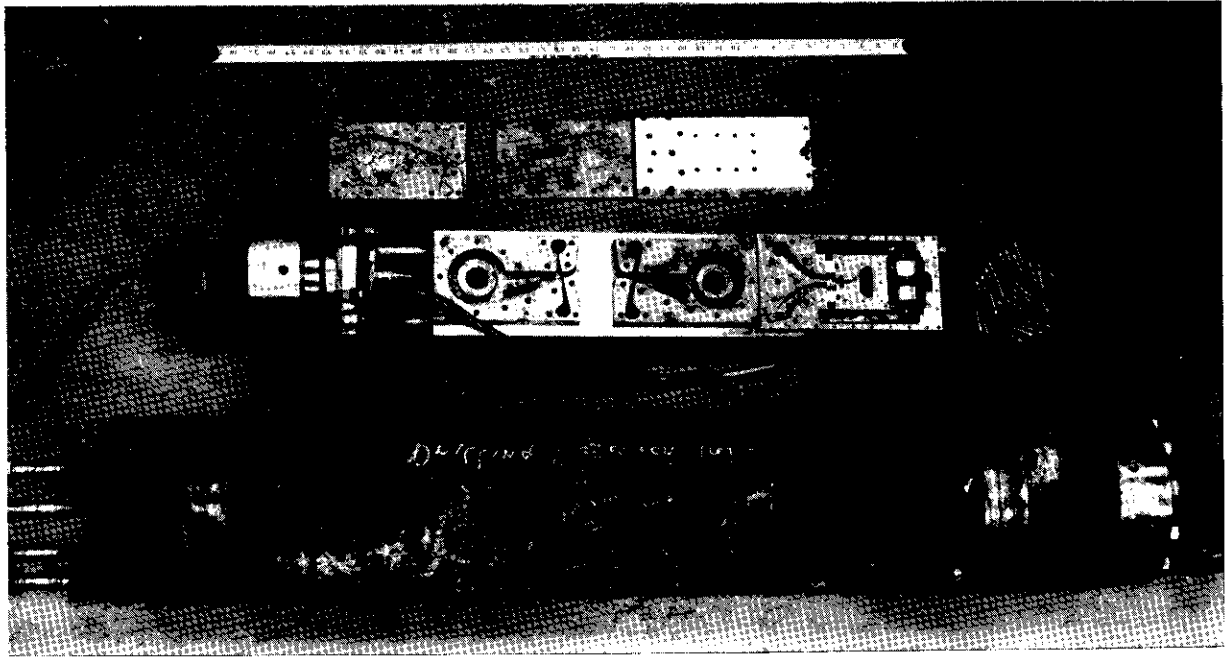


Figure 12. Amplifier-driven vortex valves, model AMP-2.

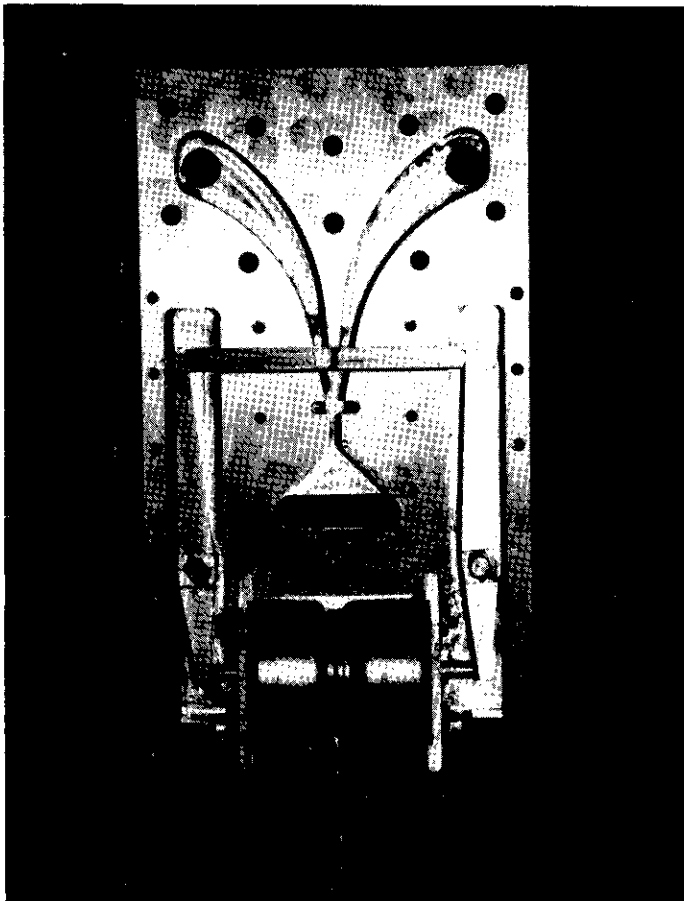


Figure 13. Solenoid actuator used in vortex valve, model AMP-2.

The actuator mechanism used with the TAB-3 model is shown in figure 16. Essentially, this mechanism is housed in a totally sealed container. Motion of the solenoid (plunger) is transmitted through the wall of the container using the flexible metal bellows described above. Pressure is compensated by a separate rubber diaphragm-type bellows (bellowfram) at the forward end of the housing. Compensation is achieved by hydraulically balancing the hydrostatic pressure of the mud on the outside of the housing with hydraulic oil in the inner area of the housing. Movement of the bellowfram also compensates for expansion and contraction of the hydraulic oil resulting from ambient temperature changes and solenoid heating.

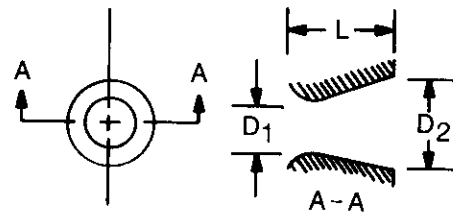


TABLE 1. NOZZLE DIMENSIONS

Nozzle	D_1	D_2	L
A	0.875	--	0
B	0.700	0.875	1.50
C	0.700	--	0
Drill bit	0.683	--	0

Note: All dimensions in inches.

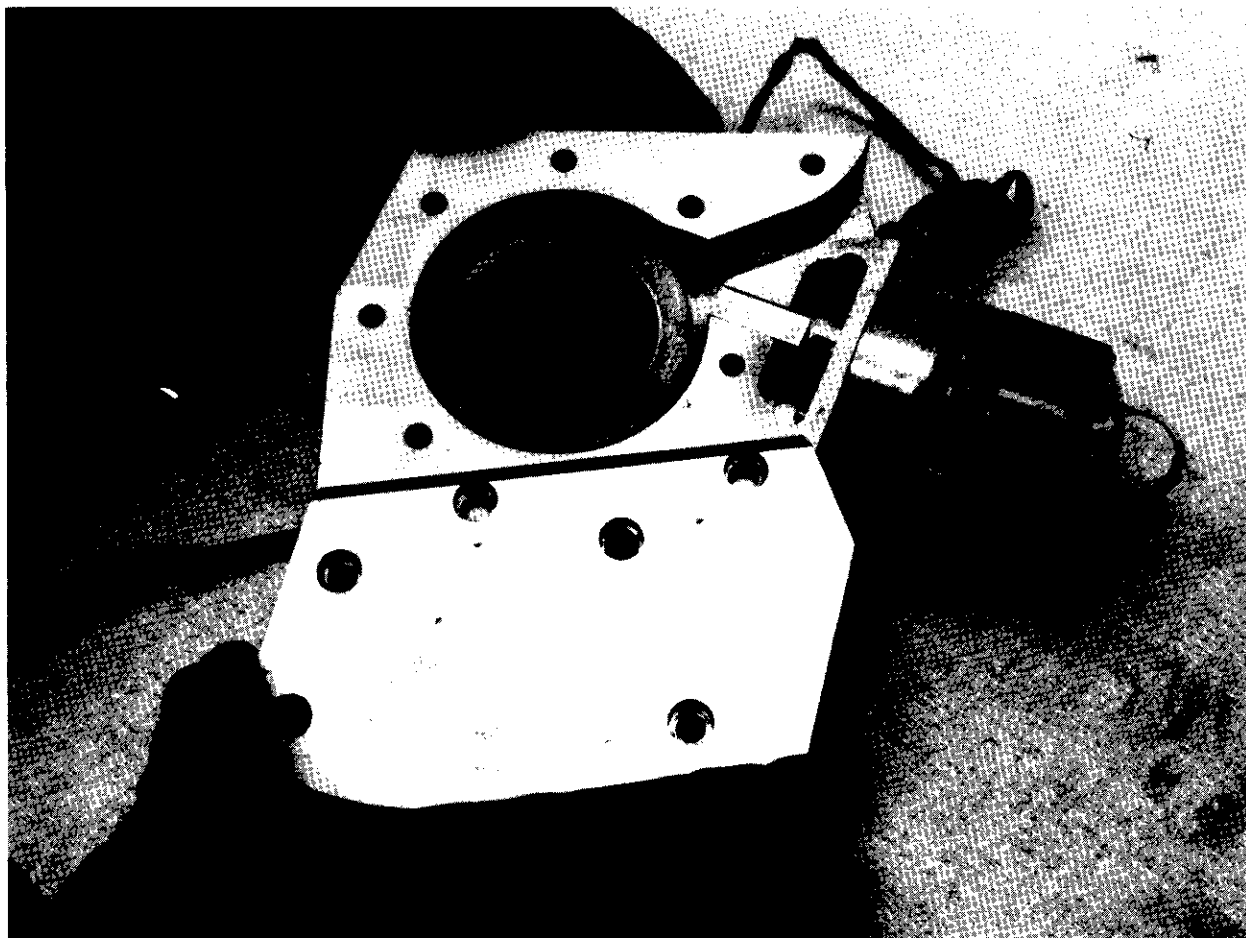


Figure 14. Tab-actuated vortex valve, model TAB-1.

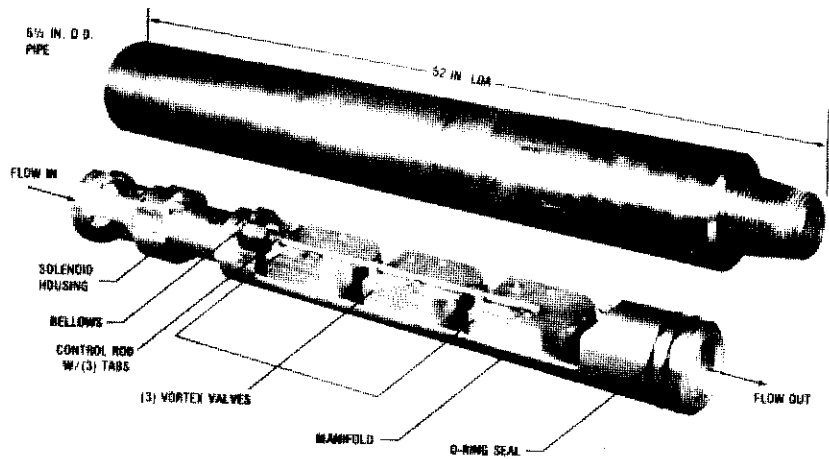


Figure 15. Tab-actuated vortex valves, model TAB-3.

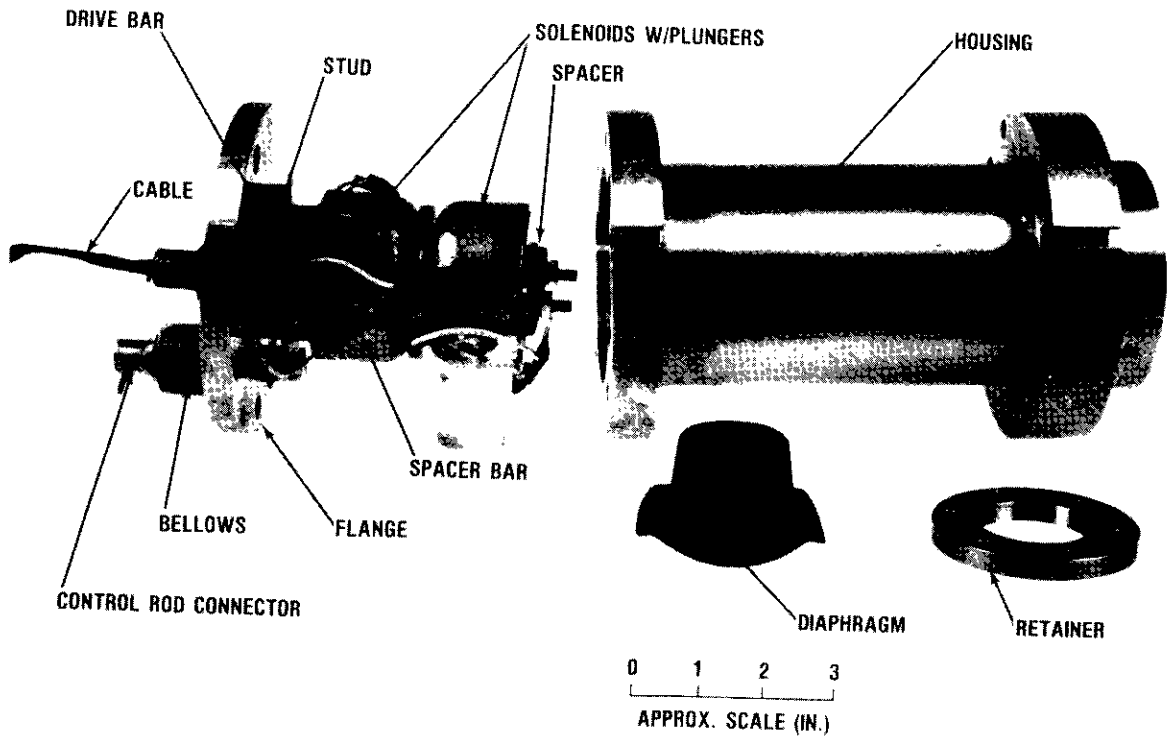


Figure 16. Actuator components.

Pressures were measured across the TAB-3 flow model with pressure taps in adapter fittings on the box and pin connections on each end of the drill pipe assembly. The internal diameter at the tap location was equal to 2.50 in. Measured pressures represented the total pressure drop across the tool.

A model containing four tab-actuated vortex valves is shown in figure 17. The valves used in this model were similar to those used in the previous (TAB-3) model. The principal difference between the models is that tungsten carbide and urethane were used to protect critical areas in the valve from abrasive drilling muds. These areas included the inner surfaces of each outlet nozzle, the upper surfaces directly above the nozzle inlets, and the surfaces directly facing the nozzle exhaust. Except for the urethane coating, which was bonded permanently to the inner surfaces of the exhaust manifold, the tungsten inserts used in the nozzles and cover plates were designed for easy replacement. Figure 18 shows the location of the inserts and associated parts used in the vortex valve assemblies. A detailed assembly drawing of this unit is shown in appendix B.

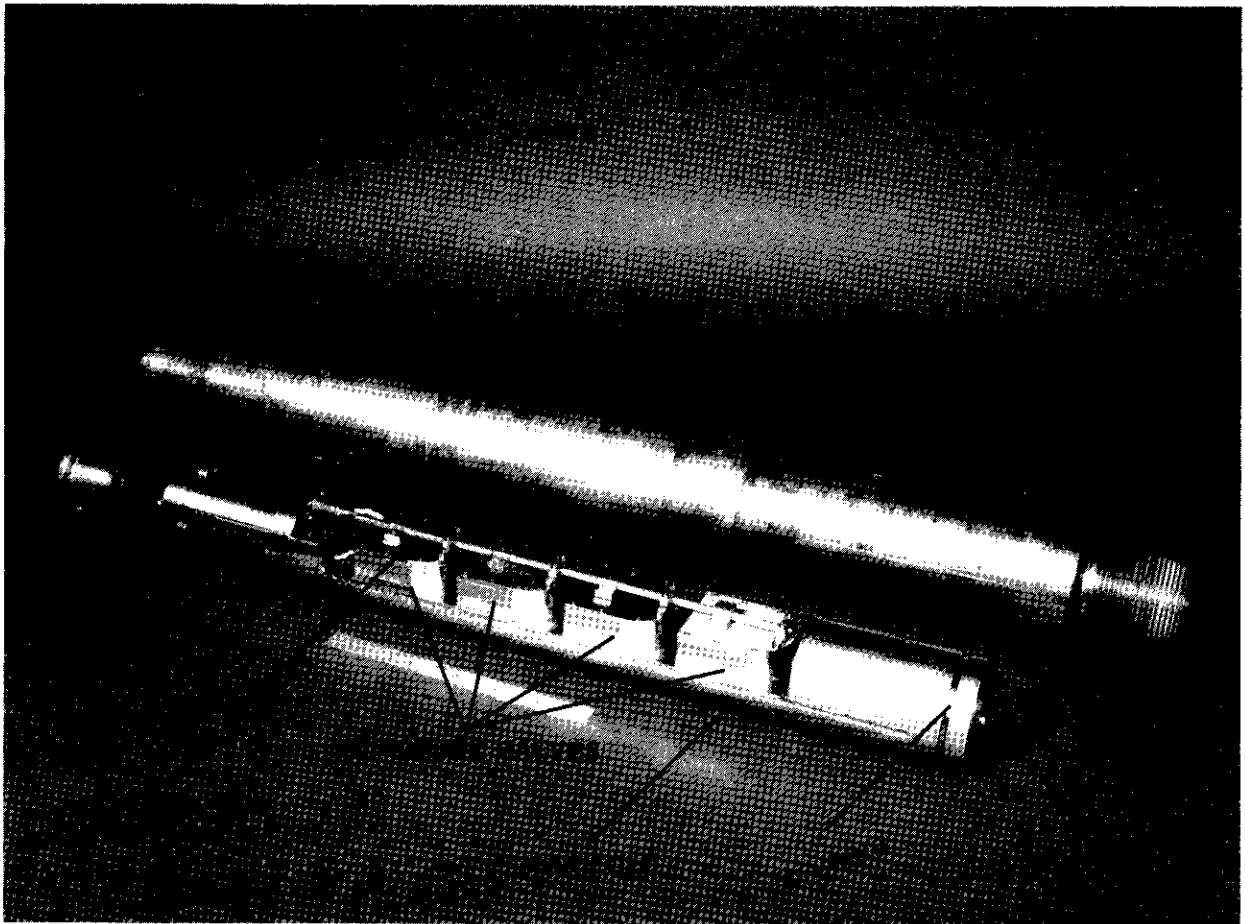


Figure 17. Tab-actuated vortex valves, **SEE FIGURE B-2, APPENDIX B** model TAB-4.

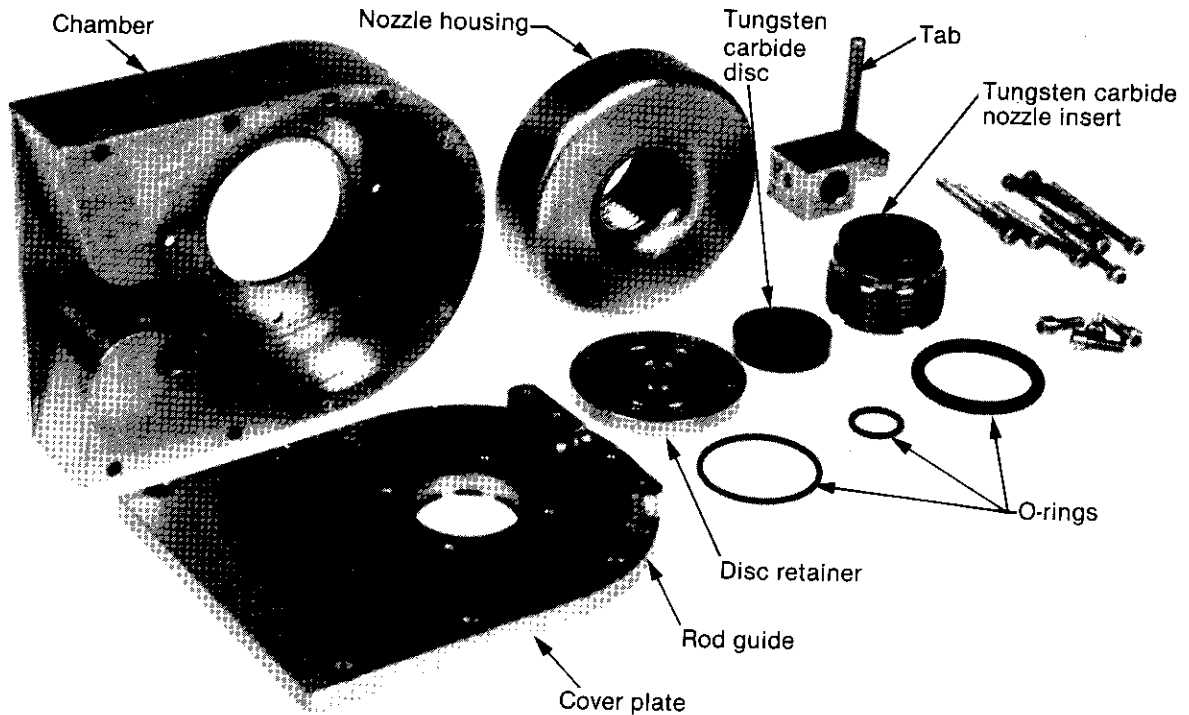


Figure 18. Vortex valve components, model TAB-4.

The TAB-4 model was actuated in a way similar to that described for the TAB-3 unit. Essentially the same actuator hardware was used. The principal difference is that a vent tube was added to equalize the pressure between the forward and aft ends of the actuator assembly to prevent pressure forces resulting from turbulence and friction along the length of the assembly from loading the pressure compensating and driving diaphragm bellows assemblies.

The TAB-4 model assembly is 54 in. long, 6¹/₂ in. in diameter, and weighs approximately 350 lb. The model was housed in the same drill pipe housing used with the TAB-3 model.

3.2 Test Fluids

The drilling muds were formulated with water as a base fluid, bentonite to build viscosity, and barite as a weighting material. The compositions of the muds are considered to represent a broad range of the types of fluids commonly used in most drilling operations. Table 2 lists mud properties used in these experiments.

3.3 Test Setups

The test setup used in the experiments conducted at HDL essentially provided a simple means to circulate a known volume of fluid between a supply

chamber and an exhaust chamber, through a model and back, using a pressure-regulated gas (nitrogen). Pressures were measured with a differential gauge connected across the model. The pressure and the time required to displace 3.01 gal. of fluid were used, along with measurements of fluid density to calculate effective flow areas. All measurements were made at a back pressure equal to approximately 300 psi to minimize cavitation. Specific details of the test setup and procedures used for the tests have been reported.⁹

TABLE 2. MUD PROPERTIES

Property	Mud I	Mud II	Mud III	Mud IV	Mud V	Mud VI
Density (ppg) ^a	8.4	12	15.3	11.9	9.1	9.8
Plastic viscosity centistokes/s ^b	11	20	27	16	15	18
Yield point (lb/100 ft ²) ^c	8	19	6	3	8	9
Gel strength (lb/100 ft ²)						
10 s	7	30	23	1	2	2
10 min	28	85	51	3	3	3

$$^a(\text{ppg})119.8 = (\text{kg}/\text{m}^3)$$

$$^b(\text{cps})10^{-3} = (\text{Pa}\cdot\text{s})$$

$$^c(\text{lb}/100 \text{ ft}^2)0.4788 = (\text{Pa})$$

A schematic diagram of the DRL test setup is shown in figure 19. Basically, in this setup a Triplex mud pump is used to circulate fluid through the flow model. Typical fluid supply pressures and delivery rates ranged from 1000 to 2000 psi and 100 to 500 gal./min (gpm). Flow rates were measured using the standard drillers' method of counting pump strokes. Pressures were measured on the inlet side of the drill pipe chamber, directly across the chamber, and on the outlet side of the chamber as indicated in the figure. During all tests the pressure on the outlet side of the model was maintained above 500 psi to minimize cavitation. In addition, a pulsation damper and a bypass choke were used to maintain the pressure produced by the vortex from exceeding 600 psi as a safety measure. Figure 20 shows a pulser being inserted into the drill pipe housing and the mud pump used in the setup.

Signals for actuating the pulser solenoids were provided by a 32-Vdc power supply operating in conjunction with an electronic (square wave) signal generator and transistorized switching circuit. Essentially, the system provided the means to operate the pulser model with variable frequency 24-V 4-A input control signals.

⁹A. Holmes and S. Gehman, *Fluidic Approach to the Design of a Pulser for Borehole Telemetry While Drilling*, Harry Diamond Laboratories, HDL-TM-79-21 (August 1979).

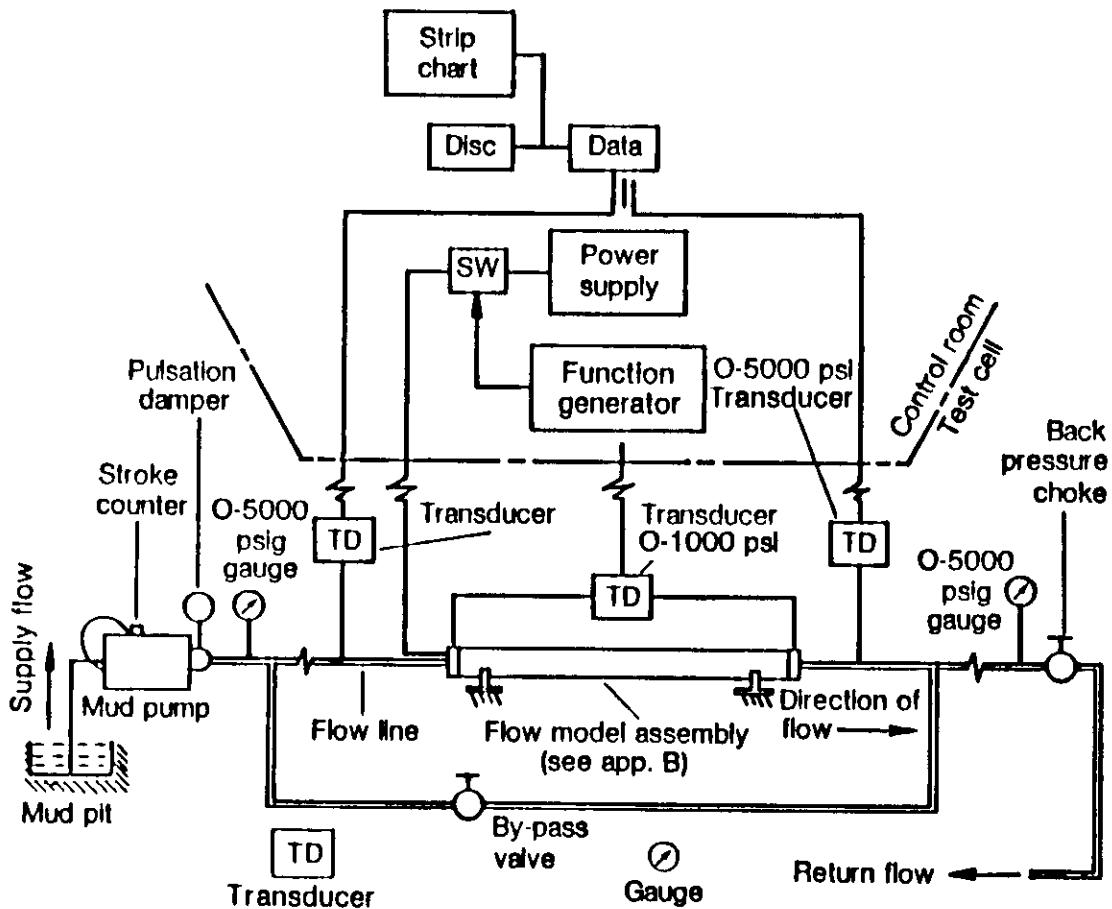
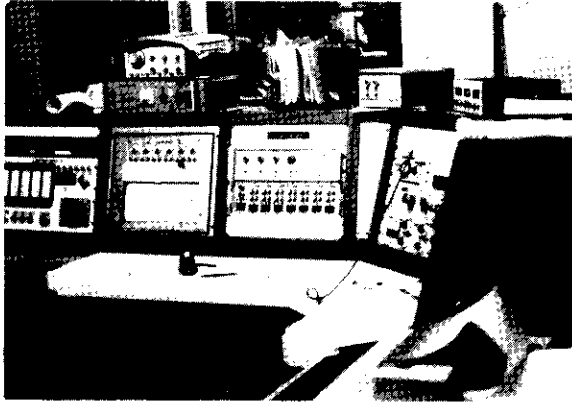


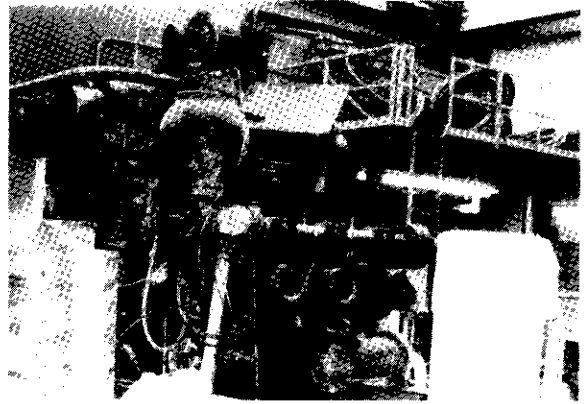
Figure 19. Drilling Research Laboratories, test setup.

During a typical steady flow experiment, a flow model was first operated in the radial flow mode at a constant flow rate while pressures were recorded for approximately 10 s. This procedure was then repeated with the model operating in the vortex flow mode. Similar procedures were followed at different flow rates. The differential pressure and flow rate were then used to calculate effective flow areas for each operating mode.

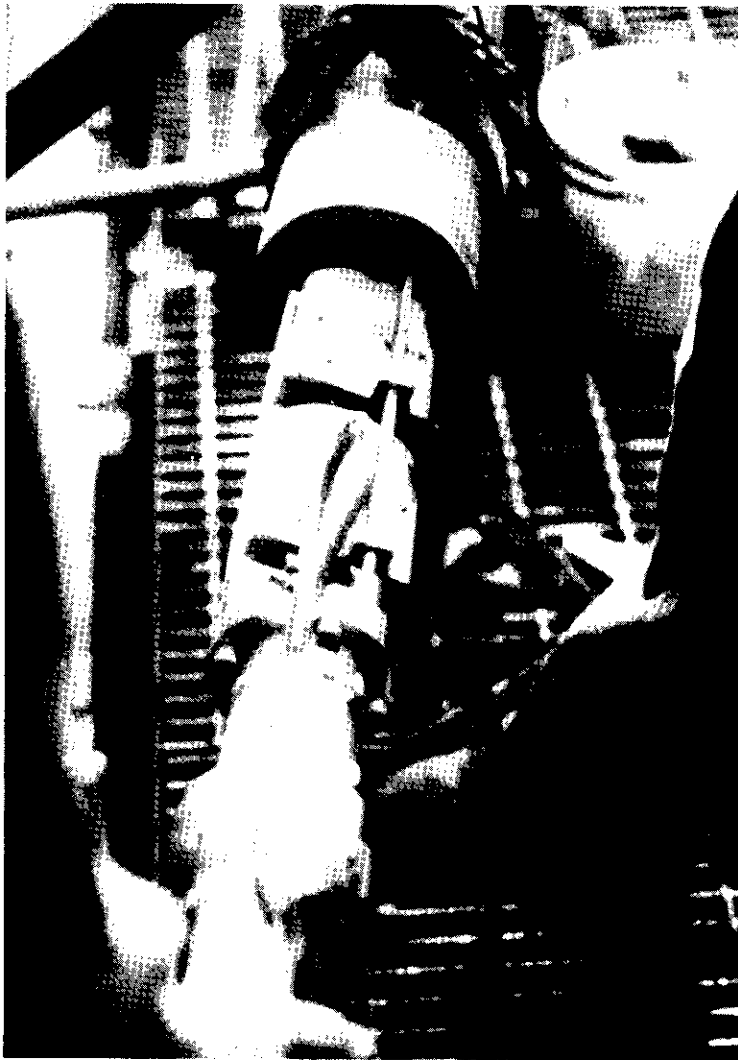
Pulsar response was measured at a constant pumping rate, but because of the pulsation damper, the actual flow rate through the model was not constant. This means that the initial change in pressure (measured while switching rapidly between the vortex and radial flow modes) cannot be correlated with pressures produced across the model at constant flow. During a typical test the control solenoids were energized with a variable frequency (28-V) signal. The change in pressure produced by the throttling action of the vortex was recorded as a function of time.



(a)



(b)



(c)

Figure 20. Drilling Research Laboratories, test setup:
(a) control room, (b) mud pump,
(c) model installation.

4. RESULTS

The purpose of the initial fluidic pulser investigations was to see how well a fluid-amplifier-driven vortex valve would throttle the types of fluids commonly used while drilling. In preliminary experiments, steady flow throttling characteristics were measured while different drilling muds and water were circulated through flow models at a constant flow rate. These measurement data were then used to calculate effective outlet nozzle flow areas and operating turndown ratios from each model and nozzle combination. Results from a number of flow tests were presented in figures 21 through 23. Average effective flow areas and operating turndown ratios from all tests are presented in table 3.

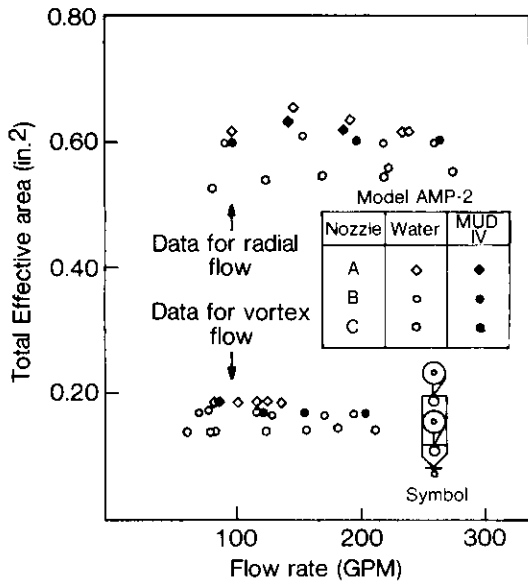


Figure 21. Effective flow area versus flow rate data describing AMP-2 model operating with vortex flow and radial flow.

Figure 23. Effective outlet area versus flow rate calculated for model TAB-1 operating with vortex and radial flow.

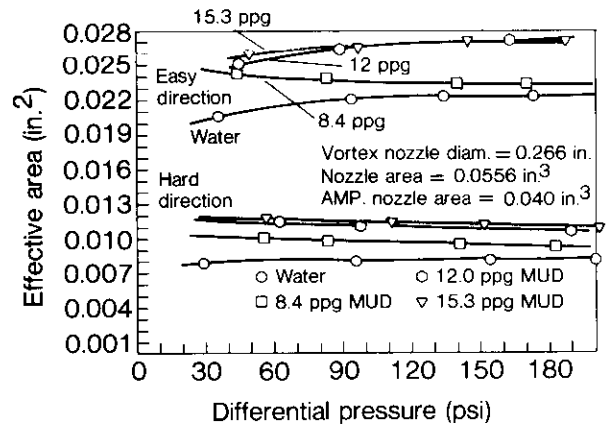


Figure 22. Effective outlet area versus supply pressure calculated for model AMP-1 operating with vortex and radial flow (from HDL-TM-79-21, reference 9).

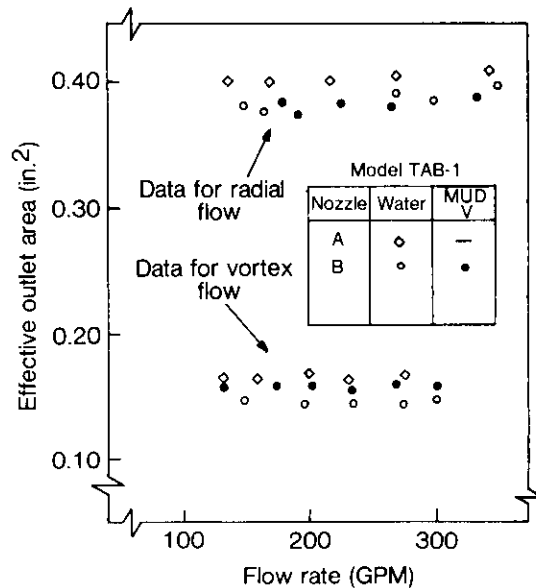


TABLE 3. SUMMARY OF FLUIDIC PULSER TEST DATA

Model No.	Nozzle type	No. used	Total port area (in. ²)	Effective port area (in. ²)	C _d	TDR	Response (Hz)	Flow rate (gpm)	Fluid
AMP-1	Convergent	1	0.055	0.022	0.400	2.7	—	—	H ₂ O
AMP-1	Convergent	1	0.055	0.024	0.430	2.4	—	—	Mud I
AMP-1	Convergent	1	0.055	0.035	0.640	2.3	—	—	Muds II, III
AMP-1T	Convergent	1	0.055	—	—	—	33	—	H ₂ O Mud III
AMP-2	A	2	1.20	0.620	0.526	3.4	3	200	H ₂ O Mud IV
AMP-2	B	2	0.770	0.604	0.784	3.8	3	200	H ₂ O Mud IV
AMP-2	C	2	0.770	0.544	0.706	4.1	3	200	H ₂ O Mud IV
TAB-1	A	1	0.600	0.403	0.671	2.5	8	125	H ₂ O Mud IV
TAB-1	B	1	0.770	0.395	1.02	2.7	8	125	H ₂ O Mud IV
TAB-3	B	3	1.155	0.807	0.70	1.62	9	450	H ₂ O Mud V
TAB-4	Drill bit	4	1.484	1.068	0.720	2.4	10	500	H ₂ O Mud VI

Examination of the data shows that throttling characteristics of the flow models were virtually unaffected by mud properties over the range of viscosity and mud weights investigated. The flatness of the curves shown in figures 19 and 20 shows that the effective resistance (area) of the outlet ports used in the models remained essentially constant with changes in flow rate. The data also show that relatively small changes (increases) in effective flow areas were produced when the viscosity of the working fluid was increased.

An examination of table 3 shows that the turndown produced by the amplifier-driven valves was always somewhat higher than that exhibited by the TAB-driven units (3.8/1 as compared to 2.7/1). The higher turndown is attributed to the increased vorticity which is produced in the vortex chamber when flow enters the chamber in a direction tangent to its centerline.

An examination of the steady flow discharge characteristics with radial flow in the chamber shows that the TAB-1 model exhibited a lower resistance to flow than the amplifier-driven units. This reduction in resistance is attributed to not having the pressure losses normally associated with the amplifier.

An examination of data pertaining to nozzles used in the vortex chambers shows that some improvements in performance (increases in discharge coefficient) were produced when a conical diffuser was used downstream of the outlet orifice (see data on nozzle B). It was also of interest that nozzle B exhibited a discharge $C = 1.2$ when operated with the chamber cover plates removed and that the discharge coefficient was reduced to $C = 1.0$ when the cover plates were used. The difference is attributed to the pressure which is being lost due to friction and turbulence in the chamber.

Steady flow discharge characteristics of the TAB-3 and TAB-4 models are summarized in table 3. An examination of these data shows that the discharge coefficients of the nozzles used in the models were somewhat lower than those determined for the same nozzles when used in the AMP-2 and TAB-1 models. The difference, in this case, is attributed to the additional pressure losses in channels and connections leading to and from the model. In the case of the AMP-2 and TAB-1 tests, the pressures were measured directly across an individual vortex valve assembly. In the TAB-3 and TAB-4 tests, the pressures were measured between the inlet and exhaust connections to the drill pipe containing the vortex valve assemblies. In the latter case, the total pressure drop across the tool is measured rather than the pressure drop across an individual valve. This therefore accounts for the additional pressure losses which occurred across inlet and exhaust connections, as well as manifolding pressure losses in the tool.

The film strip of figure 24 shows the flow exhausting from an amplifier-driven vortex valve containing two tangential inlets. During a photo sequence, a mechanically driven piston was used to actuate the amplifier controls while high-speed movies were made of the changing exhaust flow during reversal of the vortex. Results from this sequence and other photographic sequences made with water and drilling muds at 60 psi show that the vortex reversal took approximately 60 ms and that the properties of the drilling muds (muds I, II, and III) had no significant effect on the time it took to produce vortex reversal.

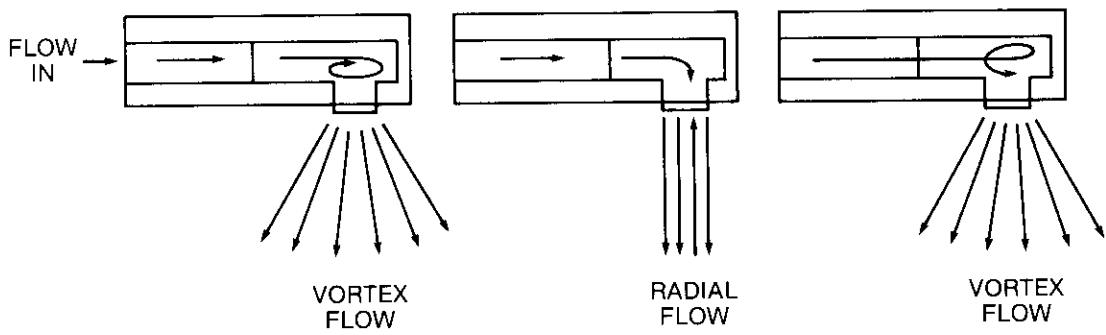
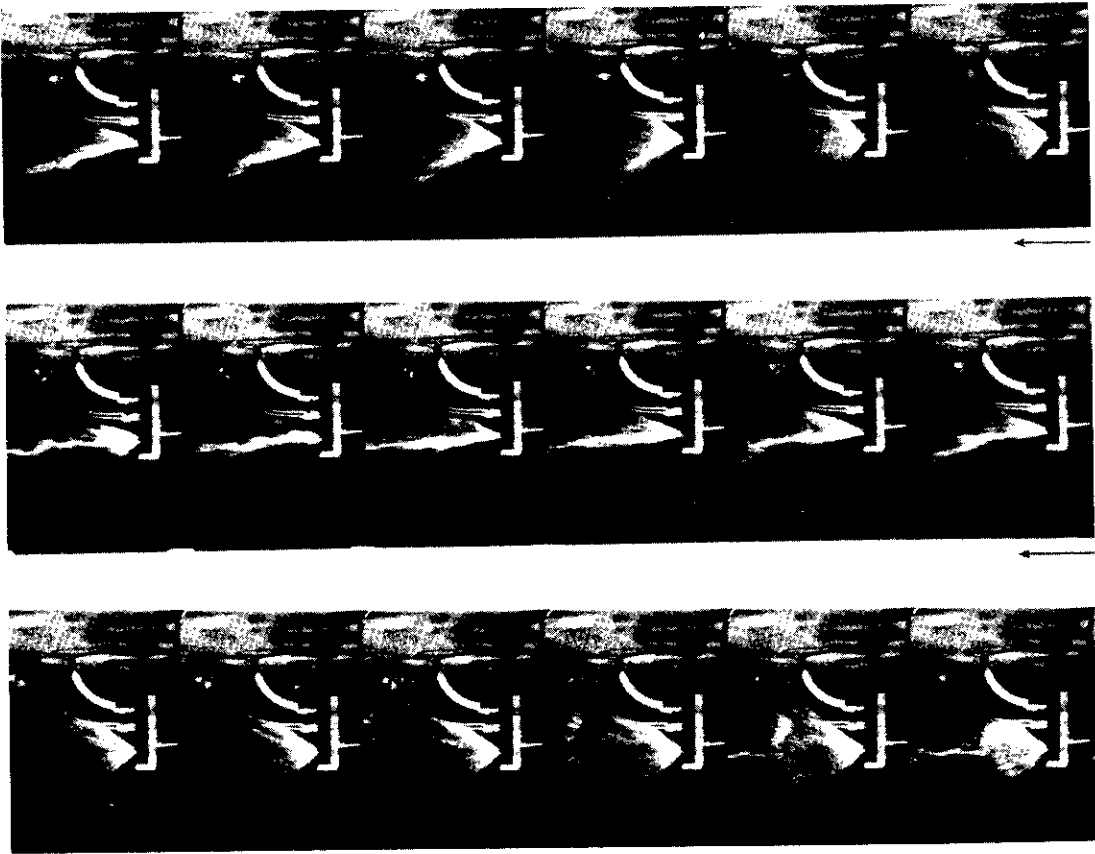


Figure 24. Photo sequence showing flow exhausting from fluid-amplifier-driven vortex valve with two tangential inlets (model AMP-1 T) during reversal of vortex.

Figure 25 describes the combined response of the amplifiers and vortex valves used in the AMP-2 flow model. During this test, the total flow rate was held constant at 250 gpm. Rise of the pulse refers to the time required to generate the vortex. Decay of the pulse describes the time required to dissipate the vortex. Pulse rise and decay time shown in the figure are equal to 0.04 and 0.18 s, respectively.

An analysis of the response data on the AMP-2 flow model showed that in all cases the risetime of the pulse was shorter than the decay time by almost a factor of 10. This unexpected result led to the conclusion that the vortex valve was loading the amplifier. This was

later confirmed when flow visualization studies using dye-injected matching and a single amplifier-driven vortex valve with a transparent cover plate showed that the amplifier power jet simply resisted being separated from the wall of the amplifier due to the high pressures which are produced in the radial amplifier outlet during vortex rotation. It was further concluded that response might be improved by using a modified amplifier geometry, but no attempt was made to do so in the present design.

Figure 26 contains a typical pressure trace showing the time required to produce and dissipate a vortex in a tab-actuated vortex valve (TAB-1) operating at 130 gpm. Rise and decay times of the pulse shown in the figure are equal to approximately 15 and 35 ms, respectively.

Figure 27 describes the response of three tab-actuated vortex valves operating with a 12-lb/gal drilling mud at a flow rate equal to 300 gpm. The pulsing frequency indicated in the figure is equal to 6 Hz.

Figure 28 describes the response of the TAB-3 model to a constant frequency (8-Hz) voltage signal when operating with water flowing at a rate equal to 400 gpm. Upon completion of these tests, the model was operated continuously at a frequency of 6 Hz for a period of 4 hr. After approximately 4 hr the model malfunctioned. An examination of the model showed that fatigue cracks had developed in the stainless-steel bellows, the pressure-compensating diaphragm had ruptured, and mud had penetrated the chamber and jammed the solenoid mechanism. Based on the amount of mud present in the housing (about a cup), it was concluded that there must be a sizeable pressure difference between the forward and rear ends of the solenoid housing which forced mud into and through the housing. In addition, a slight amount of erosion was also observed in the vortex chamber cover plate near the outlet nozzle. A

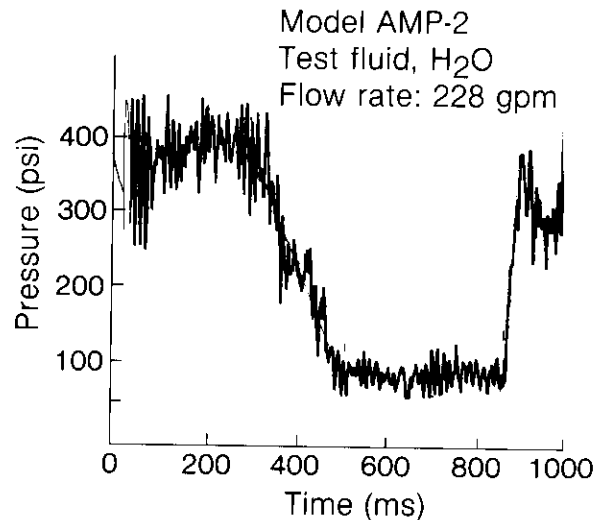


Figure 25. Response of AMP-2 pulser model to square-wave input signal when operating with water flowing at 300 gpm.

small amount of erosion was indicated by a burnishing of the vortex chamber cover plates, and an unsymmetrical swirl pattern created by material which had been removed on one side of the throat of the outlet nozzles.

Figure 29 shows the response of the TAB-4 model to a single short-duration (70 ms) pulse applied across the coils of the actuating solenoids. Corresponding rise and decay times are equal to approximately 15 and 30 ms, respectively, as indicated in the figure.

Figure 30 illustrates the response of the TAB-4 flow model to a variable-frequency input voltage signal. Maximum average frequency indicated in this figure is equal to approximately 10 Hz. Pressure traces shown in figure 31 refer to the pressure measured immediately upstream of the vortex valve (upper trace) and the pressure across the vortex valve (lower trace). Results of this and similar tests using drilling muds showed that complete switching between the radial and vortex flow modes was achieved at flow rates and operating frequencies to 500 gpm and 10 Hz. The results of the tests also showed that the maximum response of the vortex valves used was primarily limited by the electromechanical response characteristics of the actuator.

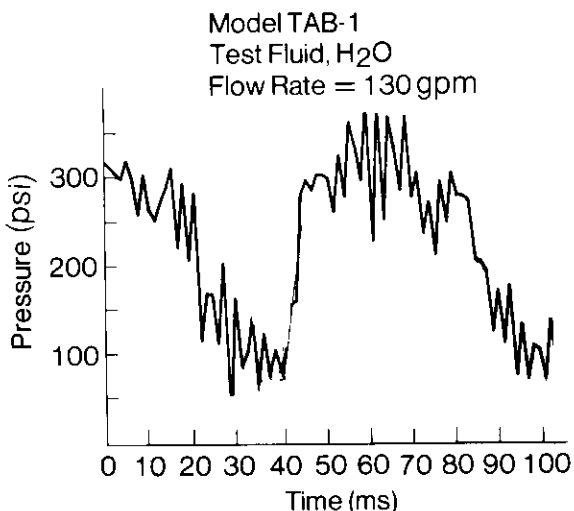


Figure 26. Response of TAB-1 model to square-wave input signal.

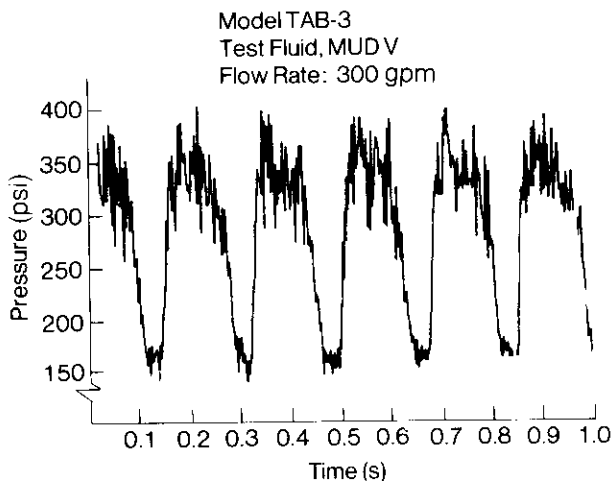


Figure 27. Response of TAB-3 model to continuous 6-Hz signal when operating with 12-ppg mud flowing at 300 gpm.

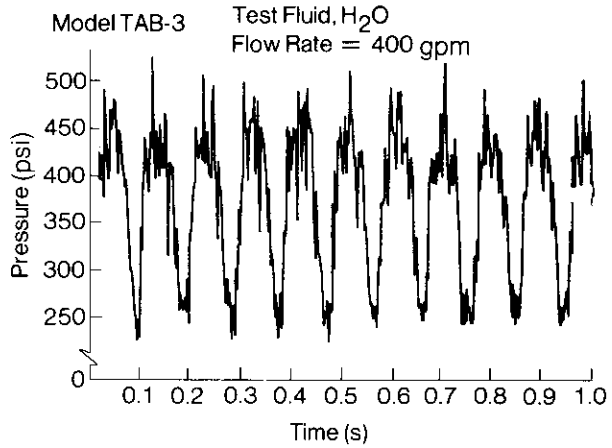


Figure 28. Response of TAB-3 model to continuous 8-Hz square-wave input signal when operating with water flowing at 400 gpm.

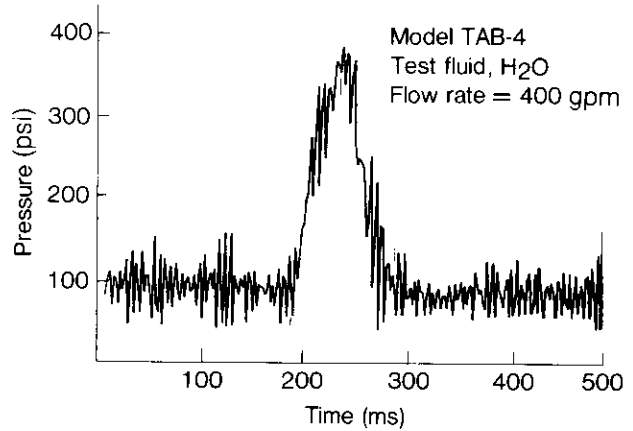


Figure 29. Response of TAB-4 model to single square-wave input pulse when operating with water flowing at 400 gpm.

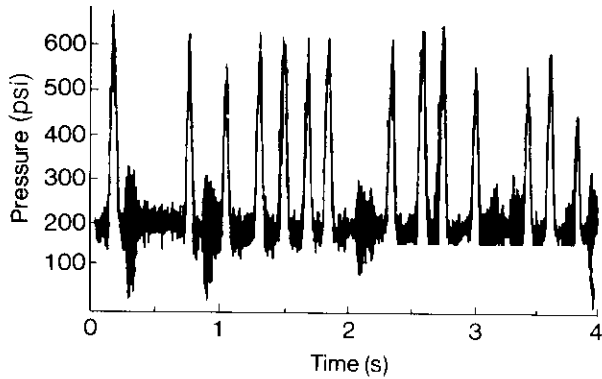


Figure 30. Response of TAB-4 model to variable frequency (DC to 10 Hz) input signal when operating on MUD VI at 300 gpm.

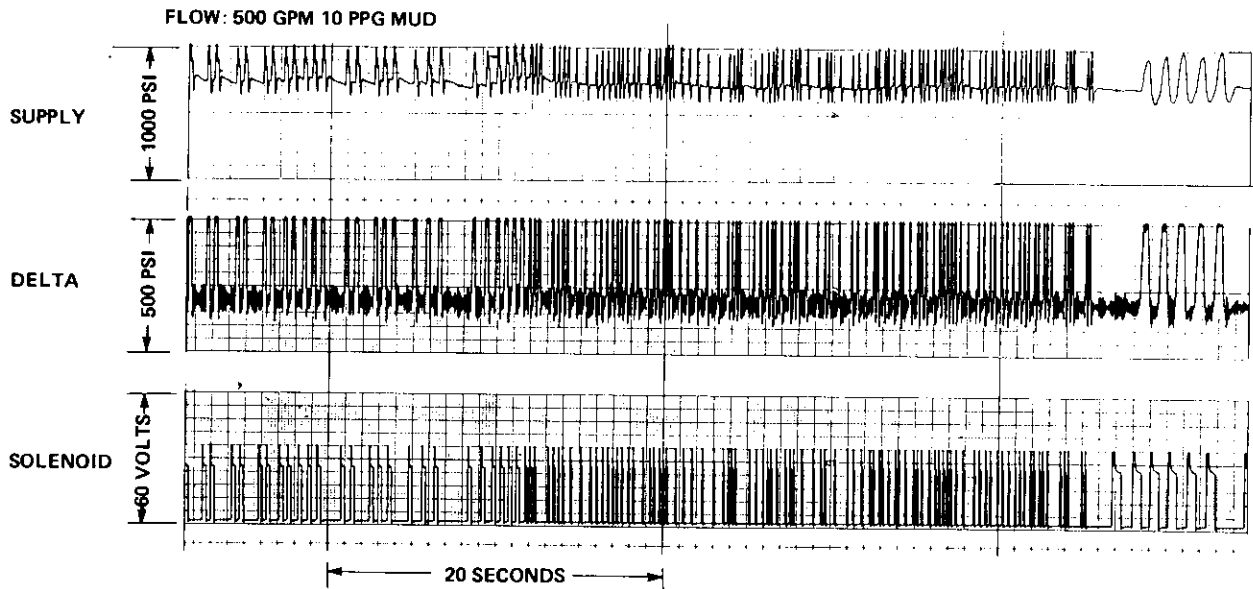


Figure 31. Response of TAB-4 model to variable frequency input signal when operating with water flowing at 500 gpm.

5. SUMMARY AND CONCLUSIONS

Three fluidic approaches to the design of a mud pulser have been investigated.

During these investigations it was shown that the capacity of a fluidic mud pulser depends upon the size and number of vortex valves used. It was also shown that the response of a fluidic mud pulser is independent of the number of individual valves used as long as the flow rate through each of the valve chambers remains the same. The results of tests also showed that the properties of the drilling muds had very little effect on the operation of flow models under the conditions stated. Based on the results of these experiments, the following points have therefore been concluded.

(1) The functional characteristics of a fluidic vortex type of mud pulsing valve will not be adversely affected by the properties of the fluids normally used in most drilling operations.

(2) Of the mud pulser valve concepts investigated, the vortex valve using tab actuation appears to be the most suited for the applications requiring high pulsing rates.

(3) A tab-actuated type of fluidic mud pulser valve consisting of eight vortex valves identical to those used in the TAB-4 flow model should be able to provide repetitive and nonrepetitive pulses at average pulsing rates to 15 Hz when operating at a flow rate equal to 1000 gpm.

6. RECOMMENDATIONS

Based on the results of the fluidic mud pulser research investigations conducted thus far, the following points are recommended:

(1) The signal analysis techniques developed during the early part of this program which describe the theoretical relationships between effective valve port areas, operating turndown ratio, signal pressure, and operating pressure drop should be expanded to include an analysis of the effects of mud rheology and drill string geometry on signal propagation characteristics

(2) It is further recommended that the present mud pulser test hardware be adopted for use as a function generator and used to study the effects of pulse frequency and mud properties on signal distortion, attenuation, and dispersion in a drill pipe.

ACKNOWLEDGEMENTS

The author acknowledges the contributions of Stacy E. Gehman to the early design, analysis, and testing of the fluidic mud pulser. Thanks are also extended to Coleman Porter, Bernard Foster, and John Bowersett for their many helpful suggestions during the design and fabrication of test hardware.

SYMBOLS AND ABBREVIATIONS

A	real outlet area
A_1	effective outlet area without vortex flow
A_2	effective outlet area with vortex flow
C_D	area correction coefficient
P_1	pressure at outer radius of chamber
P_2	pressure at radius of outlet
P_C	control pressure
P_S	supply pressure
Q_C	control flow
Q_O	outlet flow
Q_S	supply flow
r_1	chamber radius
r_2	outlet radius
v	tangential velocity

LITERATURE CITED

- (1) Drilling Technology MWD Update: New Systems Operating, Oil and Gas Journal (17 March 1980).
- (2) R. F. Spinnler and F. A. Stone, Mud Pulse Logging While Drilling Telemetry System Design, Development, and Demonstrations, Teleco Oil Field Services, Inc., Transactions of the 1978 Drilling Technology Conference, International Association of Drilling Contractors (IADC), Houston, TX (March 1978).
- (3) P. Seaton, Andrew Roberts, and L. Schoonover, Drilling Technology Update: New MWD-Gamma System Finds Many Field Applications, Oil and Gas Journal (21 February 1983), 80-83.
- (4) Marvin Gearhart, Mud Pulse MWD (Measurement-While-Drilling Systems), Society of Petroleum Engineers, SPE, 100053, 1980.
- (5) Carl W. Buchholz, Continuous Wave Mud Telemetry (The Analyst/Schlumberger) Proceedings, Technologies for MWD, Symposium, National Academy Press, Washington, DC (October 1981).
- (6) J. K. Vennard, Elementary Fluid Mechanics, 3rd Edition, John Wiley and Sons, NY (1954).
- (7) D. N. Wormley, A Review of Diode and Triode Static and Dynamic Design Techniques, Massachusetts Institute of Technology, Proceedings of the 1974 Fluidic State-of-the-Art Symposium, Vol I, Harry Diamond Laboratories, Washington, DC.
- (8) S. S. Fineblum, Vortex Diodes, State of the Art of Fluidics Symposium, Harry Diamond Laboratories (1974).
- (9) A. Holmes and S. Gehman, Fluidic Approach to the Design of a Pulser for Borehole Telemetry While Drilling, Harry Diamond Laboratories, HDL-TM-79-21 (August 1979).

Selected Bibliography--Patents

Fluidic Mud Pulser, U.S. Patent Number 4,323,991, dated 6 April 1982.

Fluid Oscillator, U.S. Patent Number 4,291,395, dated 22 September 1981.

Fluidic Pulser, U.S. Patent Number 4,276,943, dated 7 July 1981.

Electro Fluidic Actuator, U.S. Patent Number 4,391,299, dated 5 July 1983.

Fluidic Mud Pulse Telemetry Transmitter, U.S. Patent pending.

Fluidic Valve & Pulsing Device, U.S. Patent Number 4,418,712, dated 6 December 1983.

Appendix A.--Theoretical Relationships Between Vortex Valve Port Area,
Turndown Ratio, Signal Pressure, and Average Pressure Drop



A-1. SUMMARY

In the following section we describe the equations which govern the amplitude of the signals and pressure drops which are produced by series and parallel pulsing systems. In this analysis, it is assumed that the pressure on the discharge side of the drill bit nozzle remains constant and that the pulses produced by the valve occur fast enough so that an individual pulse does not have sufficient time to travel to the pump and back at the speed of sound before the next pulse is produced. It is further assumed that the inertial properties of the pump and compliance of the drill pipe cannot follow the rapid changes in pressure produced by the valve.

In the analysis, six equations are used to describe the change in pressure across the pulser, the change in pressure representing the signal (due to water hammer), and the pressure drop across the bit which occurs due to a change in flow rate. The equations are then solved for the change in flow rate. The change in flow rate is then used to calculate the signal pressure due to water hammer and the average pressure drop across the valve.

A-2. ANALYSIS

When a flow restricting device such as a vortex valve or a mechanical valve is operated in series with the nozzles in the drill bit, a positive pressure pulse is produced each time the fluid is restricted, and the pulse is ended when this restriction is removed (see fig. A-1). The restriction causes a change in the average velocity of flow in the drill pipe along with a change in pressure. When the restricting action is produced rapidly, the pressure pulse is produced by an effect commonly called water hammer. The change in pressure can be viewed as the force per unit area required to slow down the incoming flow. This change in pressure is calculated using the equation for water hammer given in Marks Handbook as

$$Q_1 - Q_2 = -K(P_1 - P_2) \quad , \quad (A-1)$$

where Q_1 and P_1 are the high resistance pressure and flow rate and Q_2 and P_2 are the low resistance pressure and flow rate. Proportionality constant $K = A/\rho c$, where A is the area of the drill pipe, ρ is the density of the circulating fluid, and c is the velocity of sound in the fluid. When the amount of time the valve is operated in the vortex mode equals the time the valve spends in the nonvortex mode, the operating duty cycle, on time/on time + off time, equals 50 percent and the average flow rate, Q_A , equals $(Q_1 + Q_2)/2$ or

$$2Q_A = Q_1 + Q_2 \quad . \quad (A-2)$$

APPENDIX A

Pulser pressure drop:

$$Q_1^2 = K_1^2(P_1 - P_{B1}) \quad \text{with vortex} \quad (A-3)$$

$$Q_2^2 = K_2^2(P_2 - P_{B2}) \quad \text{without vortex} \quad (A-4)$$

Bit pressure drop:

$$Q_1^2 = K_3^2(P_{B1}) \quad \text{with vortex} \quad (A-5)$$

$$Q_2^2 = K_3^2(P_{B2}) \quad \text{without vortex} \quad (A-6)$$

For each operating condition,

$$K_1 = A_1 \sqrt{27\rho} \quad ,$$

$$K_2 = A_2 \sqrt{27\rho} \quad ,$$

$$K_3 = 0.952A_3 \sqrt{27\rho} \quad ,$$

and P_{B1} , P_{B2} are the pressures between the pulser and the bit. When the effective areas A_2 and A_1 of the valve, average flow rate Q_A , and area of the nozzle in the bit A are specified, the coefficient 0.952 is the standard discharge coefficient used in hydraulics tables for the actual area A_3 of the bit nozzle and equations (A-1) through (A-6) uniquely describe the flow rates and pressures at the pulser and the bit.

Solving equations (A-1) through (A-6) for Q_2 gives

$$Q_2 = \frac{-b + \sqrt{b^2 - 4ac}}{2a} \quad , \quad (A-7)$$

where

$$a = (1/K_2^2) - (1/K_1^2) \quad ,$$

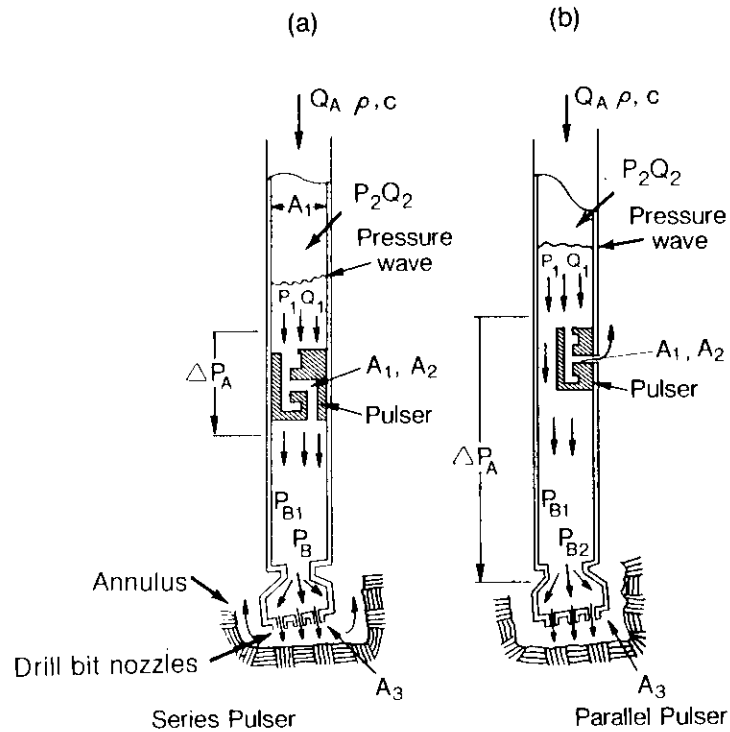
$$b = (2/K) + (4Q_A/K_1^2) \quad , \text{ and}$$

$$c = -[(4Q_A^2/K_1^2) + (2Q_A/K)] \quad ;$$

$$(1/K_1^2) = (1/K_1^2) + (1/K_3^2) \quad ,$$

$$(1/K_2^2) = (1/K_2^2) + (1/K_3^2) \quad .$$

Substituting values for Q_2 into equations (A-1) through (A-6) gives corresponding values for Q_1 , P_1 , P_2 , P_{B1} , and P_{B2} .



- A = Cross-section area of drill pipe
- A_1 = Effective outlet area with a vortex
- A_2 = Effective outlet area without a vortex
- A_3 = Area of drill bit nozzle
- C = Velocity of sound in drilling fluid
- K = Constant
- P_1 = Local pressure with a vortex
- P_2 = Local pressure without a vortex
- P_{B1} = Bit pressure with a vortex
- P_{B2} = Bit pressure without a vortex
- ΔP_A = Average pressure drop across the pulser
- Q_1 = Local flow rate with a vortex
- Q_2 = Local flow rate without a vortex
- Q_A = Average flow rate or pump rate

Figure A-1. Vortex pulser operating (a) in series with the nozzles in the drill bit and (b) in parallel with the nozzles in the drill bit.

APPENDIX A

If it is also assumed that the amount of time a vortex valve spends operating in the vortex flow mode equals the amount of time spent operating in the radial flow mode, the valve can be said to be operating on a 50-percent duty cycle (time on/time on + time off = 0.5). Under this condition, the average pressure drop across the valve is simply equal to one-half the sum of the pressure drops produced in each operating mode or

$$\Delta P_A = 1/2(Q_1^2/K_1^2 + Q_2^2/K_2^2) \quad . \quad (A-8)$$

When a fluidic or a conventional-type pulsing valve is operated in parallel with the nozzles in the drill bit, the valve is cycled open and closed and a small portion of the circulating flow is vented into the annulus through a port in the wall of the drill pipe (see fig. A-1). As the flow through the valve increases, the velocity of flow in the drill pipe increases, which causes the pressure upstream of the valve to drop. A negative wave (pressure reduction) is formed where the transition takes place, and a positive wave is formed when the valve recloses and the vent flow is zero. The duration of the resulting pulse depends upon the length of time the fluid is being vented.

The amplitude of the pressure wave or pulse, average pressure drop across the pulser, and drill bit nozzle and vent flow rate can be determined from equations (A-1) through (A-8) as follows.

If it is assumed that the pulser valve operates on a 50-percent duty cycle, the average flow through the valve can be written as $A_2/Q_2 (A_2 + C_d A_3)$, where C_d is the nominal discharge coefficient published in the Hydraulic Tables for standard drill bit nozzles. However, since the vent flow Q_2 is usually only a small portion of the total circulating flow (about 10 percent in most applications), the average flow through the valve can be approximated in terms of the average flow through the drill pipe as delivered by the mud pump:

$$\text{Average valve flow rate} = \frac{A_2 Q_A}{2(A_2 + C_d A_3)} \quad .$$

Since the average flow area exhibited by a pulser operating in parallel with nozzles in the drill bit is seldom if ever greater than 20 percent of the total drill bit nozzle area because of bottom hole cleaning considerations, the average flow rate through the drill bit nozzles can be approximated to within one percent:

$$\text{Average drill bit flow rate} = Q_A \left[1 - \frac{A_2}{2(A_2 + 0.952 A_3)} \right] \quad ,$$

where $C_d = 0.952$ is the discharge coefficient published for a standard drill bit nozzle operating at a specified flow rate.

The amplitude of the signal pulses produced by venting flow into the annulus is given by equation (A-1) in the previous section. The duration of the signal pulse is as determined by the length of time the flow is vented. For an amplifier-driven vortex valve with tangential inlets [see fig. A-2(b)], the duration of the pulse is equal to the turnaround time of the vortex, which is approximately (neglecting viscosity effects) equal to twice the volume of the chamber derived by the venting flow rate.

The above equations have been solved and used to illustrate the relationship between vortex valve turndown ratio and effective valve size on the signal pressures and average operating pressure drops which will be produced in a circulating system under a typical set of drilling conditions. For example, it is assumed that the pulser valve is to be used in series with nozzles in the drill bit as shown in figures A-1 and A-2(a).

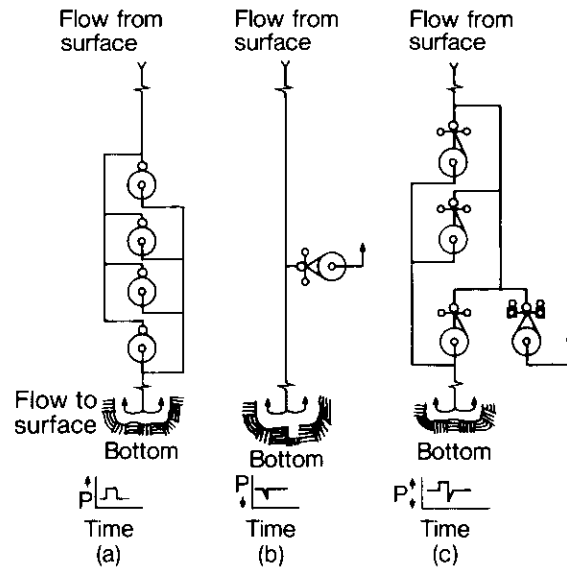


Figure A-2. Fluidic mud pulsing circuits for producing (a) positive, (b) negative, and (c) N-shaped waves.

Initial conditions

A	Drill pipe size	4.5 in. OD × 3.75 in. ID
A_3	Drill bit nozzle area	0.036 sq. in.
C_d	Drill bit nozzle discharge coefficient	0.94
Q_A	Average circulation rate	400 gpm
ρ	Mud weight	10 ppg
c	Acoustic velocity	4800 fps

The amplitude of the signal pressures and the magnitude of the average operating pressure drop which will be produced in the circulating mud system are tabulated for various valve sizes (total effective flow areas) and operating turndown ratios between 1.5/1 and 4/1 in table A-1.

APPENDIX A

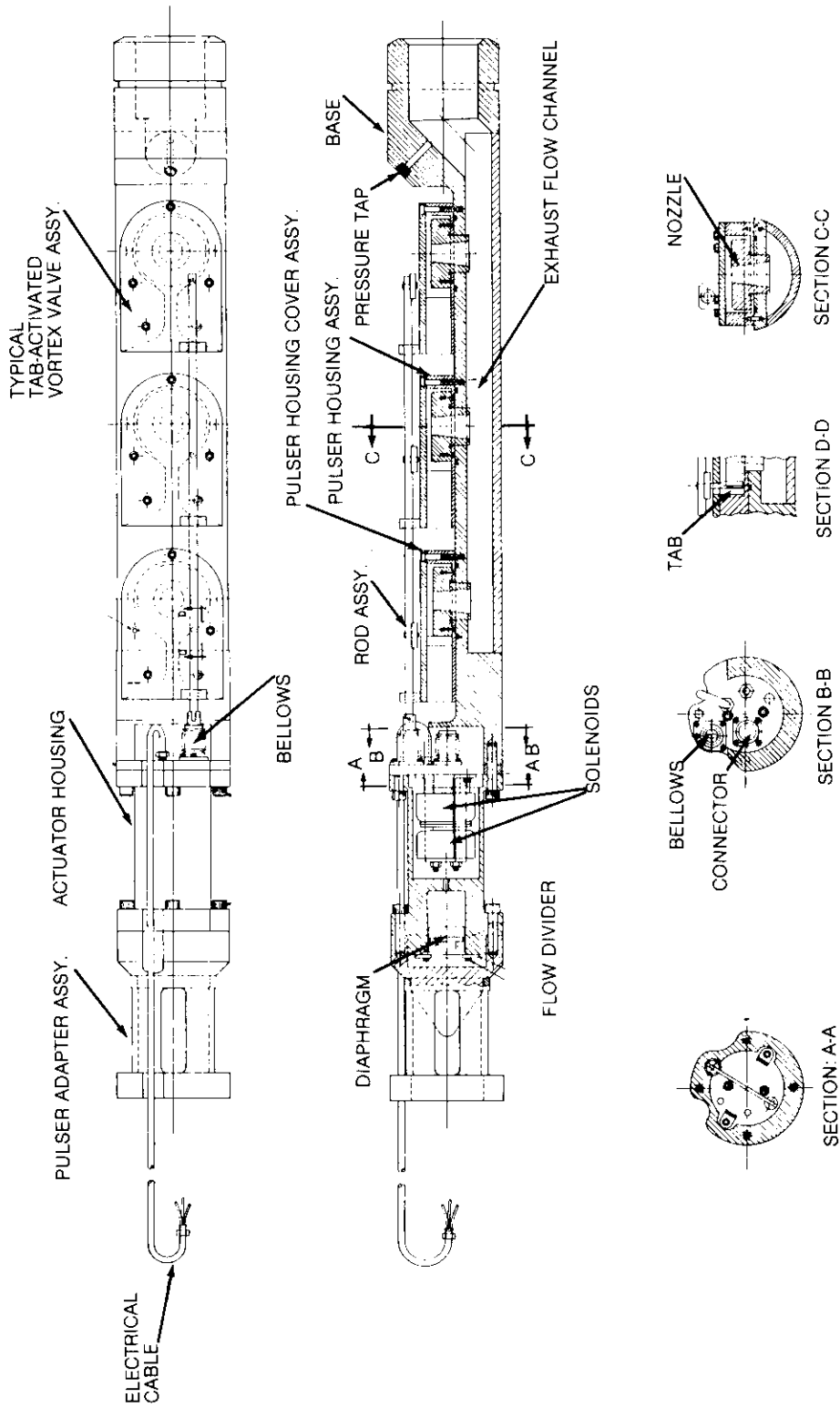
TABLE A-1. THEORETICAL SIGNAL PRESSURES AND AVERAGE PRESSURE DROPS FOR VARIOUS PULSER OUTLET AREAS AND OPERATING TURNDOWN RATIOS

A ₂	Turndown Ratio A ² /A ₁											
	1.5		2.0		2.5		3.0		3.5		4.0	
	P _S	ΔP _A	P _S	ΔP _A	P _S	ΔP _A	P _S	ΔP _A	P _S	ΔP _A	P _S	ΔP _A
1.00	47	211	107	309	173	417	241	531	309	645	376	755
1.25	32	136	73	202	122	278	174	362	228	448	283	536
1.50	23	94	53	142	89	198	130	262	173	329	218	399
1.75	17	69	40	105	68	148	100	197	135	251	172	308
2.00	13	53	31	81	53	115	79	154	107	198	138	244
2.25	10	42	25	64	43	91	64	123	87	159	113	198
2.50	8	34	20	52	35	74	52	101	72	131	94	164
2.75	7	28	17	43	29	62	44	84	61	109	79	137
3.00	6	23	14	36	25	52	37	71	51	92	67	117

Note: Calculations are based on an average flow rate Q_A = 400 gpm and a mud weight of 10 ppg.

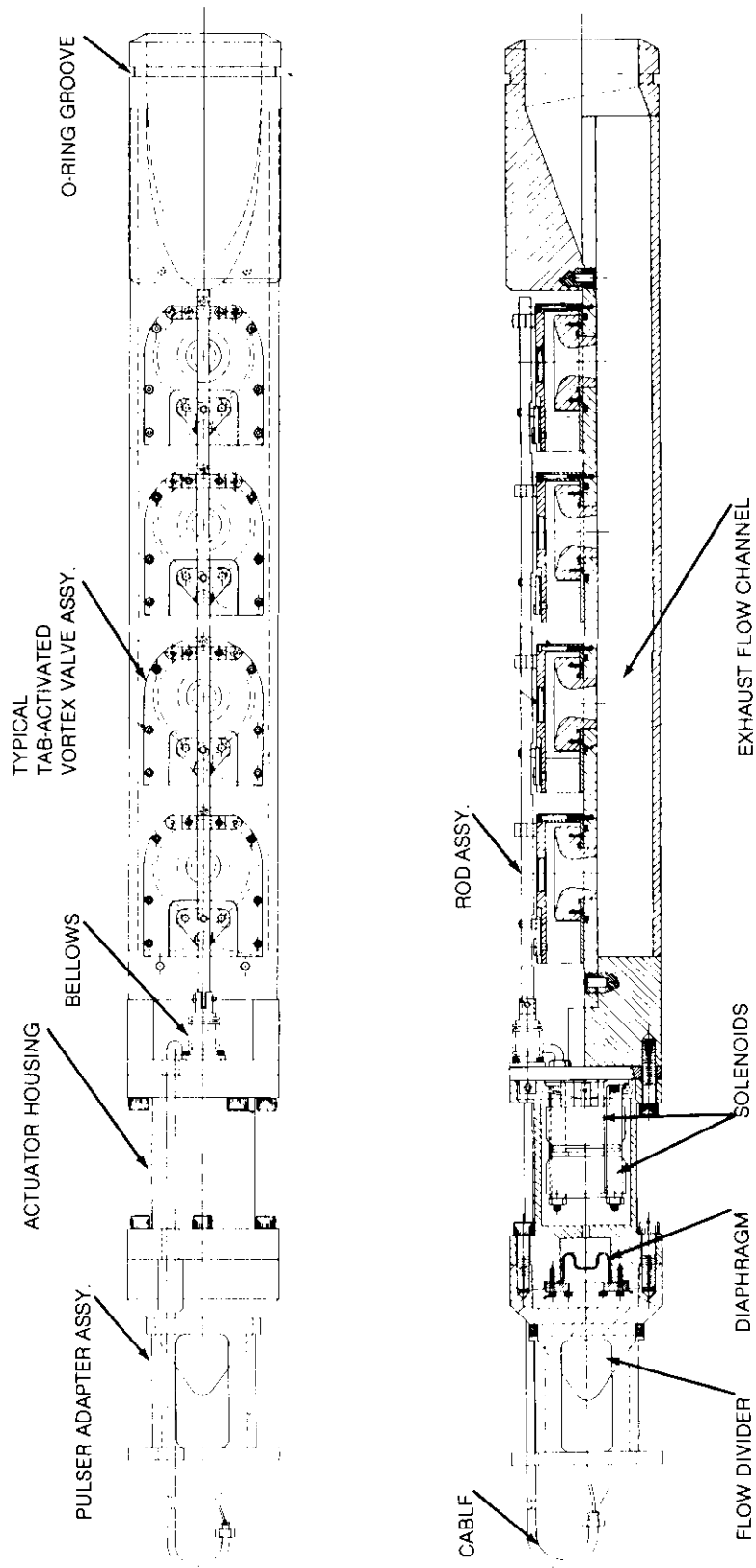
APPENDIX B.--FLUIDIC PULSER ASSEMBLY DRAWINGS, MODELS TAB-3 AND TAB-4





Note: For clarity, drill pipe housing is not shown.

Figure B-1. TAB-3 assembly



Note: For clarity, drill pipe is not shown.

Figure B-2. TAB-4 assembly

DISTRIBUTION

ADMINISTRATOR
DEFENSE TECHNICAL INFORMATION CENTER
ATTN DTIC-DDA (12 COPIES)
CAMERON STATION, BUILDING 5
ALEXANDRIA, VA 22304-6145

DEPARTMENT OF THE INTERIOR
MINERALS MANAGEMENT SERVICE
ATTN JOHN B. GREGORY (100 COPIES)
RESTON, VA 22092

COMMANDER IDDR&E
PENTAGON, ROOM 3D 1089
ATTN G. KOPCSAK
WASHINGTON, DC 20310

SMD ADVANCED TECHNOLOGY CENTER
PO BOX 1500
ATTN J. PAPADOPOULOS
HUNTSVILLE, AL 35807

COMMANDER
US ARMY FOREIGN SCIENCE
& TECHNOLOGY CENTER
FEDERAL OFFICE BUILDING
ATTN DRXST-SD1
ATTN DRXST-IS3, C. R. MOORE
220 7TH STREET, NE
CHARLOTTEVILLE, VA 22901

COMMANDER
US ARMY MISSILE COMMAND
ATTN REDSTONE SCIENTIFIC INFORMATION
CENTER, DRSMI-RBD
ATTN DRSMI-RG, WILLIAM GRIFFITH
ATTN DRSMI-TGC, J. C. DUNAWAY
ATTN DRCPM-TOE, FRED J. CHEPLEN
REDSTONE ARSENAL, AL 35898

COMMANDANT
US NAVAL POSTGRADUATE SCHOOL DEPARTMENT
OF MECHANICAL ENGINEERING
ATTN CODE 69 Nn(NUNN)
MONTEREY, CA 93940

DIRECTOR
AF OFFICE OF SCIENTIFIC RESEARCH
ATTN NE
BOLLING AFB, DC 20332

ARGONNE NATIONAL LABORATORY
APPLIED PHYSICS DIV, BLDG 316
ATTN N. M. O'FALLAN
9700 S. CASS AVE
ARGONNE, IL 60439

DEPARTMENT OF COMMERCE
BUREAU OF EAST-WEST TRADE
OFFICE OF EXPORT ADMINISTRATION
ATTN WALTER J. RUSNACK
WASHINGTON, DC 20230

DEPARTMENT OF ENERGY
C-156, GTN (OART)
ATTN ROBERT ROBERTS
ATTN SANDY DAPKUNAS
WASHINGTON, DC 20585

DEPARTMENT OF ENERGY
FE-22
ATTN T. K. LAU
WASHINGTON, DC 20585

DEPARTMENT OF ENERGY
F-317, GTN (COAL GASIFICATION)
ATTN JIM CARR
WASHINGTON, DC 20585

LOS ALAMOS SCIENTIFIC LAB
PO BOX 1663
ATTN FRANK FINCH, MS 178
LOS ALAMOS, NM 87545

NASA LANGLEY RESEARCH CENTER
ATTN MS 494, H. D. GARNER
ATTN MS 494, R. R. HELLBAUM
ATTN MS 185, TECHNICAL LIBRARY
HAMPTON, VA 23665

OAK RIDGE NATIONAL LABORATORY
CENTRAL RES LIBRARY, BLDG 4500N,
RM 175
PO BOX X
ATTN E. HOWARD
ATTN C. A. MOSSMAN
ATTN R. E. HARPER
OAK RIDGE, TN 37830

SCIENTIFIC LIBRARY
US PATENT OFFICE
ATTN MRS. CURETON
WASHINGTON, DC 20231

DISTRIBUTION (cont'd)

UNIVERSITY OF ALABAMA
CIVIL & MINERAL ENGINEERING DEPT
PO BOX 1468
ATTN HAROLD R. HENRY
UNIVERSITY, AL 35486

UNIVERSITY OF ARKANSAS
TECHNOLOGY CAMPUS
PO BOX 3017
ATTN PAUL C. MCLEOD
LITTLE ROCK, AR 72203

UNIVERSITY OF ARKANSAS
MECHANICAL ENGINEERING
ATTN JACK H. COLE, ASSOC, PROF.
FAYETTEVILLE, AR 72701

CARNEGIE-MELLON UNIVERSITY
SCHENLEY PARK
ATTN PROF. W. T. ROULEAU,
MECH ENGR DEPT
PITTSBURGH, PA 15213

CASE WESTERN RESERVE UNIVERSITY
ATTN PROF. P. A. ORNER
ATTN PROF. B. HORTON
UNIVERSITY CIRCLE
CLEVELAND, OH 44106

THE CITY COLLEGE OF THE CITY
UNIVERSITY OF NY
DEPT OF MECH ENGR
ATTN PROF. L. JIJI
ATTN PROF. G. LOWEN
139TH ST. AT CONVENT AVE
NEW YORK, NY 10031

CLEVELAND STATE UNIVERSITY
FENN COLLEGE OF ENGINEERING
ATTN PROF. R. COMPARIN
CLEVELAND, OH 44115

DUKE UNIVERSITY
COLLEGE OF ENGINEERING
ATTN C. M. HARMAN
DURHAM, NC 27706

FRANKLIN INSTITUTE OF THE STATE
OF PENNSYLVANIA
ATTN KA-CHEUNG TSUI, ELEC ENGR DIV
ATTN C. A. BELSTERLING
20TH STREET & PARKWAY
PHILADELPHIA, PA 19103

IIT RESEARCH INSTITUTE
ATTN K. E. MCKEE
10 WEST 35TH STREET
CHICAGO, IL 60616

JOHNS HOPKINS UNIVERSITY
APPLIED PHYSICS LABORATORIES
ATTN MAYNARD HILL
ATTN THOMAS RANKIN
ATTN JOSEPH WALL
LAUREL, MD 20810

LEHIGH UNIVERSITY
DEPARTMENT OF MECHANICAL ENGINEERING
ATTN PROF. FORBES T. BROWN
BETHLEHEM, PA 18015

LINDA HALL LIBRARY
ATTN DOCUMENTS DIVISION
5109 CHERRY STREET
KANSAS CITY, MO 64110

MASSACHUSETTS INSTITUTE OF TECHNOLOGY
ATTN ENGINEERING TECHNICAL REPORTS,
RM 10-408
ATTN DAVID WORMELY, MECH ENGR DEPT,
RM 3-146
77 MASSACHUSETTS AVENUE
CAMBRIDGE, MA 02139

MIAMI UNIVERSITY
DEPT OF ENG TECH
SCHOOL OF APPLIED SCIENCE
ATTN PROF. S. B. FRIEDMAN
OXFORD, OH 45056

PENNSYLVANIA STATE UNIVERSITY
ATTN J. L. SHEARER
215 MECHANICAL ENGINEERING BUILDING
UNIVERSITY PARK, PA 16802

UNIVERSITY OF TEXAS AT AUSTIN
DEPT OF MECHANICAL ENGINEERING
ATTN A. J. HEALEY
AUSTIN, TX 78712

THE UNIVERSITY OF TEXAS AT ARLINGTON
MECHANICAL ENGINEERING DEPARTMENT
ATTN ROBERT L. WOODS
ARLINGTON, TX 76019

DISTRIBUTION (cont'd)

BOWLES FLUIDICS CORPORATION
ATTN VICE PRES/ENGR
6625 DOBBINS RD
COLUMBIA, MD 21000

R. E. BOWLES
2105 SONDRRA COURT
SILVER SPRING, MD 20904

CONTROL SYSTEMS INNOVATION
ATTN N. F. MACIA
517 EAST ORION STREET
TEMPE, AZ 85283

FLUIDICS QUARTERLY
PO BOX 2989
ATTN D. H. TARUMOTO
STANFORD, CA 94305

FOXBORO COMPANY
CORPORATE
RESEARCH DIV
ATTN JAMES VIGNOS
ATTN J. DECARLO
ATTN JOHN CHANG
ATTN TOM KEGEL
38 NEPONSET AVE
FOXBORO, MA 02035

GARRETT PNEUMATIC SYSTEMS DIVISION
PO BOX 5217
ATTN TREVOR SUTTON
ATTN TOM TIPPETTS
ATTN C. ABBOTT
111 SOUTH 34TH STREET
PHOENIX, AZ 85010

GENERAL ELECTRIC COMPANY
SACE/RES DIVISIONS
PO BOX 8555
ATTN MGR LIBRARIES, LARRY CHASEN
PHILADELPHIA, PA 19101

NATIONAL FLUID POWER ASSOC.
ATTN JOHN R. LUEKE
DIR OF TECH SERVICES
3333 NORTH MAYFAIR ROAD
MILWAUKEE, WI 53222

SANDIA LABORATORIES
ATTN WILLIAM R. LEUENBERGER, DIV 2323
ATTN JERRY HOOD
ATTN NED KELTNER
ATTN ANTHONY VENERUSO, DIV 4742
ALBUQUERQUE, NM 87185

DEFENSE RESEARCH TECHNOLOGIES, INC
ATTN DR. T. DRZEWIECKI (2 COPIES)
15113 WATERGATE RD
SILVER SPRING, MD 20904

TRITEC, INC
ATTN L. SIERACKI (2 COPIES)
PO BOX 56
COLUMBIA, MD 21045

US ARMY LABORATORY COMMAND
ATTN COMMANDER, AMSLC-CG
ATTN TECHNICAL DIRECTOR, AMSLC-CT
ATTN PUBLIC AFFAIRS OFFICE, AMSLC-PA

INSTALLATION SUPPORT ACTIVITY
ATTN D
ATTN RECORD COPY, SLCIS-IM-TS
ATTN HDL LIBRARY, SLCIS-IM-TL (3 COPIES)
ATTN HDL LIBRARY, SLCIS-IM-TL (WOODBRIDGE)
ATTN TECHNICAL REPORTS BRANCH, SLCIS-IM-TR
ATTN S. ELBAUM, SLCIS-CC

HARRY DIAMOND LABORATORIES
ATTN D/DEPUTY CHIEFS OF STAFF (DCS)
ATTN J. CORRIGAN, SLCHD-NW-P
ATTN R. POLIMADEI, SLCHD-NW-P
ATTN C. LANHAM, SLCHD-TT (3 COPIES)
ATTN CHIEF, SLCHD-IT-R
ATTN H. HILL, JR., SLCHD-IT-RM
ATTN J. JOYCE, SLCHD-IT-R (10 COPIES)
ATTN A. HOLMES, SLCHD-IT-R (25 COPIES)





